

Wildfire and drought moderate the spatial elements of tree mortality

TUCKER J. FURNISS^{1,†}, ANDREW J. LARSON², VAN R. KANE³, AND JAMES A. LUTZ¹

¹Wildland Resources Department and Ecology Center, Utah State University, Logan, Utah 84322 USA

²Wilderness Institute and Department of Forest Management, University of Montana, Missoula, Montana 59812 USA

³School of Environmental and Forest Sciences, University of Washington, Seattle, Washington 98195 USA

Citation: Furniss, T. J., A. J. Larson, V. R. Kane, and J. A. Lutz. 2020. Wildfire and drought moderate the spatial elements of tree mortality. *Ecosphere* 11(8):e03214. 10.1002/ecs2.3214

Abstract. Background tree mortality is a complex process that requires large sample sizes and long time-scales to disentangle the suite of ecological factors that collectively contribute to tree stress, decline, and eventual mortality. Tree mortality associated with acute disturbance events, in contrast, is conspicuous and frequently studied, but there remains a lack of research regarding the role of background mortality processes in mediating the severity and delayed effects of disturbance. We conducted an empirical study by measuring the rates, causes, and spatial pattern of mortality annually among 32,989 individual trees within a large forest demography plot in the Sierra Nevada. We characterized the relationships between background mortality, compound disturbances (fire and drought), and forest spatial structure, and we integrated our findings with a synthesis of the existing literature from around the world to develop a conceptual framework describing the spatio-temporal signatures of background and disturbance-related tree mortality. The interactive effects of fire, drought, and background mortality processes altered the rate, spatial structuring, and ecological consequences of mortality. Before fire, spatially non-random mortality was only evident among small ($1 < \text{cm DBH} \leq 10$)- and medium ($10 < \text{cm DBH} \leq 60$)-diameter classes; mortality rates were low (1.7% per yr), and mortality was density-dependent among small-diameter trees. Direct fire damage caused the greatest number of mortalities (70% of stems ≥ 1 cm DBH), but the more enduring effects of this disturbance on the demography and spatial pattern of large-diameter trees occurred during the post-fire mortality regime. The combined effects of disturbance and biotic mortality agents provoked density-dependent mortality among large-diameter (≥ 60 cm DBH) trees, eliciting a distinct post-disturbance mortality regime that did not resemble the pattern of either pre-fire mortality or direct fire effects. The disproportionate ecological significance of the largest trees renders this mortality regime acutely consequential to the long-term structure and function of forests.

Key words: bark beetles; density dependence; distance dependence; drought; fire effects; forest ecology; large-diameter trees; Smithsonian ForestGEO; spatial patterns; tree mortality; wildfire; Yosemite Forest Dynamics Plot.

Received 8 May 2020; **accepted** 19 May 2020; **final version received** 15 June 2020. Corresponding Editor: Debra P. C. Peters.

Copyright: © 2020 The Authors. This is an open access article under the terms of the Creative Commons Attribution License, which permits use, distribution and reproduction in any medium, provided the original work is properly cited.

† E-mail: tucker.furniss@usu.edu

INTRODUCTION

Tree mortality is regulated by complex interactions among many physical, biological, and ecological stressors (e.g., competition; Franklin et al. 1987). These stressors operate across a wide

range of temporal and spatial scales (<0.1 to >1000 ha; Das et al. 2008, van Mantgem et al. 2009, Birch et al. 2019a) to determine the rates and causes of background mortality (Das et al. 2016). Acute disturbances (e.g., wildfire), in comparison, result in rapid and conspicuous

mortality events that can affect entire stands, landscapes, or regions (Turner et al. 1997, Meddens et al. 2012, 2018a). Disturbances are often studied in isolation from background mortality processes, but recent research indicates that these omnipresent ecological processes can alter disturbance severity and mediate delayed mortality (Hood et al. 2018, van Mantgem et al. 2018). Here, we synthesize previous research with an empirical study to develop a conceptual framework describing how background mortality processes and acute disturbance events collectively regulate tree mortality.

We first discuss the relevant literature and ecological basis regarding the spatial elements of background mortality, spatial elements of fire-related mortality, and interactions between these processes. Rather than a systematic literature review, we incorporated representative studies that serve to frame our understanding of the scales at which various ecological processes elicit spatially non-random patterns in mortality. To do this, we considered research that has explicitly addressed spatial scale, and we developed a conceptual framework describing the spatio-temporal scales at which each mortality process is most evident. We emphasized research from temperate forests of western North America to maintain relevance to the forest in which this study was conducted, but we also incorporated research from around the world to demonstrate the potential for this conceptual framework to have a broad biogeographic scope. In addition to eight studies spanning western North America and two based on global datasets, this synthesis was based on studies from the Sierra Nevada (5), Pacific Northwest (10), northeast United States and Canada (4), southwest United States (4), southeast United States (2), Rocky Mountains (2), Europe (4), northeast China (2), northern Africa (1), and Patagonia (1).

We then conduct an empirical assessment of the spatial elements of tree mortality using nine years of annual mortality among 32,989 individual trees within a large (25.6 ha), stem-mapped forest demography plot that was exposed to both fire and severe drought part way through the study period. The temporal and spatial scope of this study, combined with process-based measurements of tree mortality, renders our dataset uniquely poised to quantify the relationship

between background mortality processes, disturbance-related mortality, and forest spatial structure. Focusing on the spatial aspects of mortality and the reciprocal nature of various mortality processes (i.e., mortality refines spatial patterns, and spatial patterns regulate mortality risk), we used multiple analytical methods to empirically evaluate the annual rates, causes, and spatial elements of tree mortality during three distinct mortality regimes: (1) background (i.e., pre-fire) mortality, (2) immediate fire-induced mortality (due to direct fire damage), and (3) post-disturbance mortality (determined by the additive and interactive effects of background mortality agents, fire, and severe drought).

The spatio-temporal signature of tree mortality processes

Tree mortality processes can be described in terms of the agents of mortality, spatial scale, and temporal scale (Fig. 1A). Many mortality processes have been well-studied and quantitatively described at a range of spatial scales including insect epidemics, drought, and storm events (e.g., windthrow, ice storms). The timescale of these conspicuous mortality agents can be extremely acute (e.g., storms) or span multiple years (e.g., beetle epidemic, multi-year drought), and they create patterns in mortality that are evident at both intermediate and broad spatial scales (10–10,000 ha; Raffa et al. 2008, Allen et al. 2010, Meddens et al. 2012, 2018a, Baguskas et al. 2014). Conversely, slower-acting background mortality processes, including competition, endemic bark beetle activity, and pathogens, are more evident at finer spatial scales (<1 ha) and longer temporal scales (>3 yr; Fig. 1A). The slower dynamics of these processes makes them challenging to study, often requiring long observation periods and large plots for patterns in mortality to emerge (Clark and Clark 1996, Lutz and Halpern 2006, McMahon et al. 2019). Although subtle, background mortality processes regulate forest turnover rates in the absence of severe disturbance (van Mantgem et al. 2009), and they are important determinants of fine-scale spatial dynamics within stands (Das et al. 2008, Larson et al. 2015).

Mechanisms of spatial structuring

The ecological mechanisms that give rise to spatio-temporal patterns in tree mortality may be

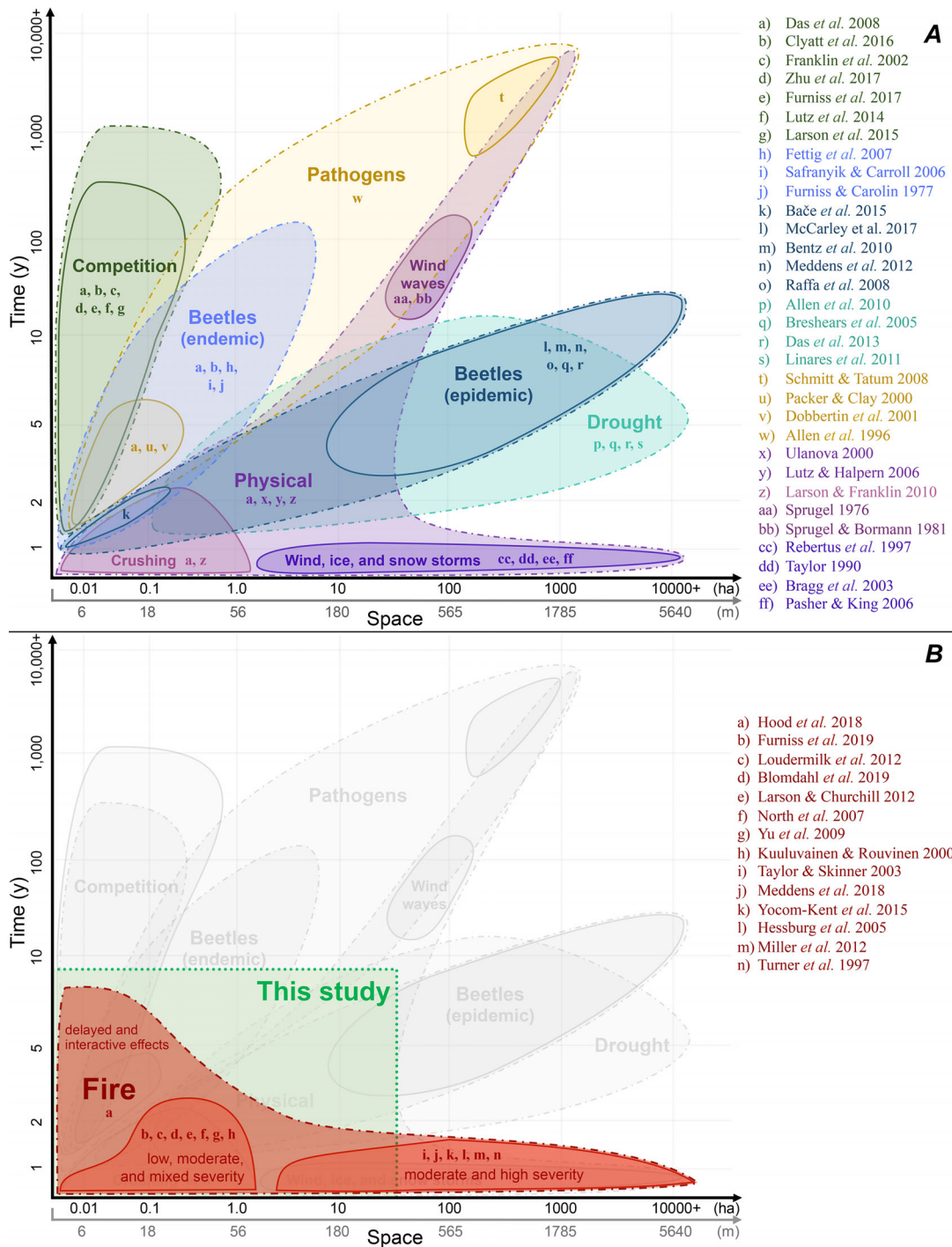


Fig. 1. Spatio-temporal scales of background tree mortality processes (A) and fire (B). Letters represent studies that have described each mortality process with explicit consideration of spatial or temporal scale; dark lines indicate the scales at which there is quantitative evidence of each process operating, while dotted lines indicate qualitative descriptions of scale. The two x-axis scales represent area-based scale in hectares (ha) on top with the corresponding linear scale (radii in m) below.

broadly grouped into three categories: density dependence, distance dependence, and environmental heterogeneity. Density-dependent mortality emerges when tree neighborhoods mediate mortality risk (Kenkel 1988, Larson et al. 2015), and is evident as elevated susceptibility to competition (Gray and He 2009, Das et al. 2011), biotic mortality agents (Janzen 1970, Packer and Clay 2000, Johnson et al. 2014), and abiotic mechanisms (King 1986, Das et al. 2008, Yu et al. 2009, Schaedel et al. 2017) in dense tree neighborhoods. Distance dependence, in contrast, refers to the elevated risk of mortality for trees close to an affected individual, a characteristic associated with many mortality agents including pathogens, insects, and crushing (i.e., contagion; Goh- een and Hansen 1993, Das et al. 2008, Raffa et al. 2008). Finally, environmental heterogeneity contributes to non-random patterns in tree mortality by introducing variability in light, water, soil resources, and habitat suitability which influence growth rate, vigor, and concomitant mortality risk (Greenwood and Weisberg 2008, Linares et al. 2011, Furniss et al. 2017). These mechanisms function simultaneously, and the spatio-temporal patterns of mortality are generally determined by a combination of all three mechanisms.

While density dependence has been used to describe patterns of both distance- and density-dependent mortality associated with competition and biotic mortality agents (e.g., insects, pathogens), we define these terms separately to decouple the distinct relationships between each mechanism and forest spatial structure. Forest spatial structure regulates density-dependent mortality directly through resource competition (Kenkel 1988), morphological constraints (King 1986), accumulation of host-specific plant enemies (Janzen 1970, Connell 1971), and by moderating trees' ability to invest in defense mechanisms (Lorio 1986, Herms and Mattson 1992, Kolb et al. 1998, Fettig et al. 2007, Hood et al. 2016, Stephenson et al. 2019). Conversely, forest spatial structure does not directly regulate distance-dependent mortality. Rather, distance-dependent mortality processes are spatially autocorrelated due simply to the contagious nature of certain mortality agents (e.g., pathogen spread, beetles dispersing from a recently killed tree).

While many mortality processes are both distance- and density-dependent, differentiating these terms is critical to understanding the ecological nuances of spatially non-random mortality processes. Distance-dependent mortality may be density-independent (i.e., mortality may be spatially autocorrelated but independent of local density), and conversely, density-dependent mortality may be distance-independent (i.e., mortality may not be spatially autocorrelated despite mortality risk being elevated in dense neighborhoods). In other words, density-dependent mortality is a pattern that emerges when forest spatial structure mediates mortality risk, while distance-dependent mortality is the consequence of autocorrelated mortality processes. This distinction may be conceptualized as opposing directions of the relationship between forest spatial structure and mortality risk: Density dependence represents the effect of forest spatial pattern on mortality risk, while distance dependence represents the effect of mortality processes on forest spatial pattern.

Spatial elements of background mortality

Perhaps the most widely recognized example of spatially structured tree mortality is competition-dominated density dependence that defines the competitive exclusion phase of forest succession models (Yoda 1963, Peet and Christensen 1987, Franklin et al. 2002). This form of density dependence is most often observed in young and even-aged forests (Kenkel 1988, Larson et al. 2015, Birch et al. 2019b), but asymmetric competition can continue to cause density-dependent mortality in mature and old-growth forests as well (Lutz et al. 2014, Furniss et al. 2017, Zhu et al. 2017). In these more structurally complex forests (Lutz et al. 2018, Jeronimo et al. 2019), mortality agents including bark beetles, pathogens, and physical damage (Franklin et al. 1987, Larson and Franklin 2010, Das et al. 2016) become increasingly important determinants of mortality, and patterns in background mortality are structured by a complex mix of both distance- and density-dependent mechanisms (Das et al. 2008, 2011, 2016, Silver et al. 2013, Gendreau-Berthiaume et al. 2016, Lintz et al. 2016).

Individual mortality agents may be both distance- and density-dependent. Bark beetles, for example, create contagious patches of mortality

(i.e., distance dependence) by releasing aggregation pheromones that attract nearby beetles to a single individual and overwhelm the tree's defenses (Raffa and Berryman 1983), and successful mass attacks result in a concentrated point source of beetles that disperse to nearby trees (Raffa et al. 2008). Density dependence further contributes to spatial patterns of beetle-related mortality as local forest structure determines the intensity of competition and thus the availability of resources necessary for trees to invest in defense chemicals and resist beetle attacks (Lorio 1986, Herms and Mattson 1992, Fettig et al. 2007, Hood et al. 2016). Density dependence is also evident at broad scales as forest composition and host tree density regulate background beetle population levels which determines success rate of mass attacks, and neighborhoods with high host tree density may be preferentially selected by dispersing beetles (Raffa and Berryman 1983, Kolb et al. 2007, Raffa et al. 2008). Patterns in bark beetle mortality can also be driven by variability in drought intensity across a landscape (Baguskas et al. 2014), as susceptibility to beetle attack is closely related to drought severity (McDowell et al. 2008, Anderegg et al. 2015).

Pathogen-related mortality is determined by a similarly complex mix of spatially structured processes. For example, the widely cited pattern of conspecific negative density dependence (CNDD; Hille Ris Lambers et al. 2002, Comita et al. 2010, LaManna et al. 2017) is often attributed to host-specific pathogen accumulation (Janzen-Connell hypothesis), but this distance-dependent contagion is reinforced by the elevated intensity of intraspecific competition (Adler et al. 2018; but also see Detto et al. 2019) near conspecific host trees (i.e., conspecific density dependence). The below-ground growth form and slow spread rate of pathogens make their contagion detectable as patches or rings of mortality that manifest at intermediate to large (1–100 ha) spatial scales (Lung-Escarmant and Guyon 2004, Schmitt and Tatum 2008), but this is generally only evident over long timescales (decades to centuries, Fig. 1A; Waring et al. 1987). The spatial elements of insect activity may also contribute to the spatial structuring of pathogens as fungal spores can be transported to new host trees by the insects themselves (Goheen and

Hansen 1993, Paine et al. 1997, Safranyik and Carroll 2006).

Finally, physical mortality agents including crushing and some forms of wind-related mortality (e.g., wind waves) may be regarded as distance-dependent as probability of mortality is positively related to the proximity to a falling tree (Das et al. 2008) or the edge of a gap (Taylor 1990). Patches of wind-related mortality are often associated with root- and stem-rot (Sprugel 1976), and their spatial structure is therefore additionally influenced by the distribution and spread of saprophytic decay fungi. Physical mortality agents that operate at broader spatial scales, such as wind, ice, and snow storms, are most strongly determined by environmental heterogeneity (Rebertus et al. 1997) and the spatial variability in the intensity of the weather event (Pasher and King 2006). The density dependence of physical mortality agents is perhaps most apparent in single-age stands where density directly influences tree morphology (i.e., diameter to height ratio) and thus resistance of trees to strong wind (King 1986). Physical mortality agents may be both positively and negatively density-dependent. Stand density can influence tree morphology (i.e., diameter to height ratio) and thus be positively related to susceptibility of trees to strong wind (King 1986), while high density stands can also ameliorate the localized intensity of wind and ice storms and thus reduce mortality risk (Bragg et al. 2003).

Spatial elements of direct fire mortality

Fire is an intrinsically spatial process, causing patterns in mortality that are both distance- (proximity to flames) and density-dependent (density alters fire behavior). Heterogeneity in fire effects introduces complex patterns across a wide range of spatial scales from <0.01 ha (Blomdahl et al. 2019) to >10,000 ha (Turner et al. 1997, Meddens et al. 2018a, Whitman et al. 2018, Fig. 1B). Fire behavior is spatially autocorrelated due to heat transfer from burning fuels to adjacent vegetation (Michaletz and Johnson 2006, 2008, Smith et al. 2016, 2017) that creates patchiness in patterns of cambial heating, crown scorch, and concomitant tree mortality (Loudermilk et al. 2012, Hood et al. 2018, Furniss et al. 2019). During surface fire, tree crowns are damaged primarily by convective heat transfer from plumes of heated air that quickly

kill foliage, buds, and vascular tissue, while tree boles are more susceptible to conductive and radiative heat transfer from combustion of surface fuels (Hood et al. 2018). The thick bark of fire-adapted species and large-diameter trees can protect from this radiative heat to some extent (van Wagten-donk and Fites-Kaufman 2006, Belote et al. 2015), but the long residence time of heat released from smoldering duff and slow burning fuels (e.g., large woody debris) can penetrate this thick bark and warm the cambium enough to cause tissue death ($\geq 60^{\circ}\text{C}$; Hood et al. 2018). By driving both fire temperature and residence time, the size and arrangement of fuels (Hiers et al. 2009, Loudermilk et al. 2012) influence both the intensity (energy release) and severity (ecological consequences) of fire (Jeronimo et al. 2020).

Weather, topography, and environmental heterogeneity can also create spatial patterns in fire effects. Areas that burn under moderate weather conditions generally burn with lower intensity compared to areas that burn under more extreme fire weather conditions (e.g., strong winds, low relative humidity; Lydersen et al. 2014). This is particularly evident during extreme weather conditions when positive feedback cycles between fire and the atmosphere create self-sustaining, plume-dominated fire behavior that results in large patches of high-severity fire effects across vast portions of a landscape (Allen 2007, Lydersen et al. 2014). Topography contributes to spatial autocorrelated fire behavior both directly through regulating fire intensity (e.g., higher intensity toward ridge tops; Turner and Romme 1994, Kane et al. 2015) and indirectly through feedbacks with forest structure (Jeronimo et al. 2020).

Forest structure regulates fire behavior at both fine (Thaxton and Platt 2006, Hiers et al. 2009, Loudermilk et al. 2012) and broad scales (Rothermel 1972, Miller and Urban 1999a, b, 2000a, Harris and Taylor 2015), and it contributes to temporal patterns by moderating fuel connectivity and regulating spread rate (Caprio and Swetnam 1995, Miller and Urban 2000b, Taylor and Skinner 2003). Conversely, repeated fire events influence the spatial pattern dynamics of trees and fuels within stands (scales <10 ha; Youngblood et al. 2004, North et al. 2007, Larson and Churchill 2012), and broad-scale patterns in fire behavior (>10 ha) create, rearrange, and refine patches of forest,

unburned islands, and early-seral habitat among stands and across broad landscapes (>1000 ha; Turner et al. 1997, Hessburg et al. 1999, Taylor and Skinner 2003, Kane et al. 2014, Meddens et al. 2018a, b, Jeronimo et al. 2019). In short, heterogeneity in forest spatial structure contributes to variability in fire intensity, and variability in fire intensity perpetuates heterogeneity in forest structure. This reciprocal relationship between fire, fuels, and forest spatial structure mediates the severity of future fires, and this self-regulation renders fire foundational to the structure and function of many forest ecosystems (van Wagten-donk and Fites-Kaufman 2006, Scholl and Taylor 2010, Larson et al. 2013).

Larson and Churchill (2012) reviewed the literature regarding spatial pattern dynamics in frequent-fire forests, and they characterized spatial patterns in these forest types as a shifting mosaic of individuals, clumps, and openings. They described the iterative nature of fire spatial pattern interactions including mechanisms of pattern formation and maintenance, and this model has become an archetype for spatial pattern dynamics in frequent-fire forests (Franklin and Johnson 2012, Hessburg et al. 2015, North et al. 2019). While this model may be sufficient to describe the feedbacks between fire and forest spatial structure, there is limited consideration of how background mortality processes interact with fire to mediate the spatial pattern dynamics in post-fire forests and to moderate mortality in between fire events.

There is extensive overlap between the spatio-temporal signature of fire and background mortality agents (Fig. 1), and this suggests that background mortality processes may be important contributors to patterns observed in post-fire mortality. There are indeed many studies of interactions between background mortality processes and fire in the literature (Hood and Bentz 2007, Youngblood et al. 2009, van Mantgem et al. 2013, 2018, Kane et al. 2017b, Hood et al. 2018, Stephens et al. 2018), but these studies are focused primarily on the nature of the interaction (i.e., amplified or inhibited; Kane et al. 2017b) rather than the interactive effects of these processes on patterns in mortality.

Spatial elements of post-fire mortality

Among the most widely studied mortality process in post-fire forests is competition for water

and soil resources. Stand structure mediates the intensity of inter-tree competition and creates heterogeneity in the severity of drought- and competition-related stress (Fensham and Holman 1999, Guarín and Taylor 2005, Allen et al. 2010, van Mantgem et al. 2016), and this modifies the susceptibility of trees to both direct (van Mantgem et al. 2013, Furniss et al. 2019) and indirect fire-related mortality (van Mantgem et al. 2016, 2018, Hood et al. 2018). While inter-tree competition in unburned forests is often considered to primarily inhibit seedlings and small-diameter trees, recent studies suggest that competition in post-fire forests can be an important determinant of mortality for larger trees as well (Yu et al. 2009, van Mantgem et al. 2018). The nature of drought–fire interactions is also dependent on the timing of events: Fire reduces stand density, and this can make surviving trees less susceptible to competition- and drought-related mortality post-fire (van Mantgem et al. 2011, 2016), but pre-fire drought can hinder trees' ability to tolerate fire damage and can increase probability of immediate fire-related mortality (van Mantgem et al. 2013, 2018).

Bark beetles have been long considered as an important factor in mediating post-fire mortality (Ryan and Amman 1996, Scott et al. 2002, Sieg et al. 2006, Hood and Bentz 2007), but the effects of local tree neighborhood on susceptibility to bark beetles are complex and dependent on a variety of post-fire factors (Kolb et al. 2007). As with beetle-related mortality in a pre-fire mortality regime, local neighborhood structure and composition influence the availability of resources necessary for trees to invest in defense infrastructure (i.e., resin and resin ducts; Hood and Sala 2015), and this directly contributes to resistance against bark beetle attack (Raffa 2014). As fire decreases density and competition for resources, we might expect fire to enhance resistance to bark beetle attack by increasing resource availability and thus the capacity of trees to invest in resin defenses. However, surviving trees may be temporarily weakened due to direct fire injury to their foliage, cambial tissue, and surface roots, and this may limit their capacity to defend against beetle attack immediately after fire (McHugh and Kolb 2003, Kolb et al. 2007). Fire may further intensify bark beetle pressure by creating an abundance of weakened host trees

across the landscape that are susceptible to beetle attack and thus enabling beetle populations to proliferate. This increase in beetle abundance may facilitate more successful mass attacks and can catalyze a transition from endemic to epidemic beetle population dynamics (Raffa et al. 2008). Empirical studies have found evidence for both facilitated and impeded bark beetle mortality post-fire (Youngblood et al. 2009, Hood et al. 2016): Fire may initially increase susceptibility to bark beetles by weakening trees and reducing their ability to defend (McHugh and Kolb 2003, Hood and Bentz 2007, Kolb et al. 2007, Youngblood et al. 2009), but fire is also thought to increase resistance to bark beetles over longer timescales by reducing stand density, increasing the distances between conspecifics, and stimulating the production of resin (Fettig et al. 2007, Hood et al. 2015, 2016).

Pathogens also interact with fire damage to mediate post-fire mortality (Parker et al. 2006, Kane et al. 2017b), and local tree neighborhoods may affect susceptibility to pathogens post-fire through altering resource availability, overall vigor, and capacity to defend against pathogens. As with bark beetles, it is not clear whether fire will enhance or reduce the prominence of pathogen-related mortality (Kane et al. 2017b). Fire may facilitate the apparent virulence of pathogens by weakening trees (Parker et al. 2006), but it may also impede pathogens (Grelen 1983, Beh et al. 2012) by scorching the soil, reducing the number of live trees, and increasing distance between suitable host trees. Three-way interactions between pathogens, bark beetles, and drought on fire-weakened trees may further complicate the detection of pathogen-caused mortality in post-fire forests.

Applications for post-fire mortality models

There is a growing body of evidence (Youngblood et al. 2009, Hood et al. 2018, van Mantgem et al. 2018, Furniss et al. 2019) that suggests that these background mortality processes play a key role in shaping post-fire mortality, but they are absent from the most widely used post-fire tree mortality models. A recent update of the First Order Fire Effects Model (FOFEM; Hood and Lutes 2017) has improved model accuracy by incorporating bark beetle presence/absence as a predictor variable for four species-specific

models (Hood and Lutes 2017), but this binary approach is not optimally suited to capture the complex nature of bark beetle population dynamics (Raffa et al. 2008). Furniss et al. (2019) found that mortality model prediction error was spatially autocorrelated, indicating that spatially structured mortality processes not only mediate patterns in post-fire mortality, they comprise some of the unexplained prediction error within fire effects models. This is supported by recent efforts to integrate background mortality agents including bark beetles, pathogens, and competition into theoretical frameworks describing the mechanisms of post-fire tree mortality at scales ranging from individual trees (Hood et al. 2018) to broad landscapes (Kane et al. 2017b).

Objectives

The considerable volume of background tree mortality literature demonstrates a variety of mechanisms by which biotic and abiotic mortality agents evoke spatial patterns in tree mortality (Fig. 1). Yet, there is not currently a cohesive framework for assessing how fire and other acute disturbance events may modify the relative importance and spatio-temporal structure of background mortality processes. We addressed this by quantifying the spatial elements of pre-fire, direct fire, and post-fire tree mortality, then developing an empirically informed framework describing how fire and background mortality processes interactively mediate mortality and collectively determine forest spatial pattern dynamics. For each mortality regime (pre-fire, direct fire, and post-fire), we examined the spatial structure of distance-dependent mortality processes using point pattern analysis, and we evaluated the intensity and spatial extent of density dependence using generalized linear models.

We tested the null hypothesis that fire and background mortality processes do not interact, resulting in a post-fire mortality regime that may be characterized simply by the additive effects of direct fire damage and background mortality processes. Alternatively, we hypothesized that fire may override and obscure background mortality processes, impeding the spatial elements of background mortality and imposing patterns in post-fire mortality that reflect only the heterogeneity in direct fire damage. In this case, we would expect the spatial patterns associated with

background mortality agents (e.g., bark beetles, pathogens) to become spatially random, or to resemble the spatial pattern of direct fire damage (e.g., crown scorch). A second alternative hypothesis is that fire may interact with background mortality processes, creating patterns in post-fire mortality that do not resemble the patterns of either pre-fire or direct fire mortality alone. Finally, we hypothesized that mortality would become less density-dependent post-fire because reduced stand density may have increased above- and below-ground resource availability, thus reducing the sensitivity of surviving trees to competitive stress and contagious mortality agents within their local neighborhoods.

METHODS

Study area

We conducted this study in an old-growth *Abies concolor*–*Pinus lambertiana* (white fir–sugar pine) forest in the lower-montane, mixed-conifer forest zone of the Sierra Nevada, California, USA. We used data from the Yosemite Forest Dynamics Plot (YFDP; Lutz et al. 2012, Lutz 2015), a 25.6-ha stem-mapped forest monitoring plot located between 1774 and 1911 m elevation in Yosemite National Park, with species composition and structure representative of the Sierra Nevada white fir superassociation (Keeler-Wolf et al. 2012). The YFDP was established in 2009 and 2010 when we tagged, identified, and mapped all tree stems ≥ 1 cm diameter at breast height (DBH; 1.37 m) within the plot ($n = 34,458$ live stems; Lutz et al. 2012). We considered four tree species comprising 32,989 stems ≥ 1 cm DBH within the YFDP: *A. concolor* [Gordon] Lindl. ex Hildebr. (white fir; 939 stems/ha), *P. lambertiana* Dougl. (sugar pine; 180 stems/ha), *Calocedrus decurrens* [Torr.] Florin (incense cedar; 64 stems/ha), and *Quercus kelloggii* Newb. (California black oak; 46 stems/ha).

Fire in the YFDP.—The YFDP has been relatively unaffected by timber harvest and grazing, but a century of effective fire suppression had a profound impact on the pre-fire structure and composition of this forest. The lack of fire resulted in an abundance of surface and ladder fuels, uncharacteristically high stem density, and a compositional shift toward shade-tolerant

species (Caprio and Swetnam 1995, Scholl and Taylor 2010, North et al. 2019). The high fuel loads associated with these stands can make the reintroduction of fire challenging (Lydersen et al. 2014), often requiring mechanical fuel reduction and prescribed fire treatments to develop historical structure, composition, and spatial pattern that confer resilience to wildfire, drought, and biotic disturbance (North et al. 2007, Safford et al. 2012, Stephens et al. 2018).

The YFDP was burned for the first time in 113 yr (Barth et al. 2015) as part of a management-ignited fire set to control the spread of the

Rim Fire, a 104,131-ha wildfire that burned in August and September of 2013. The fire was ignited ~1 km from the YFDP on 31 August 2013, and no management action was taken within the YFDP before or after ignition. Fire intensity ranged from low- to high-intensity surface fire with patches of unburned surface fuels (primarily in draws; Lutz et al. 2017a, Blomdahl et al. 2019) and occasional crown torching (Fig. 2). Surface fuel consumption was >90% for litter, duff, and small fuels (<1000 h), and 61% for coarse woody debris (Larson et al. 2016, Cansler et al. 2019). Fire effects were heterogeneous with patches of

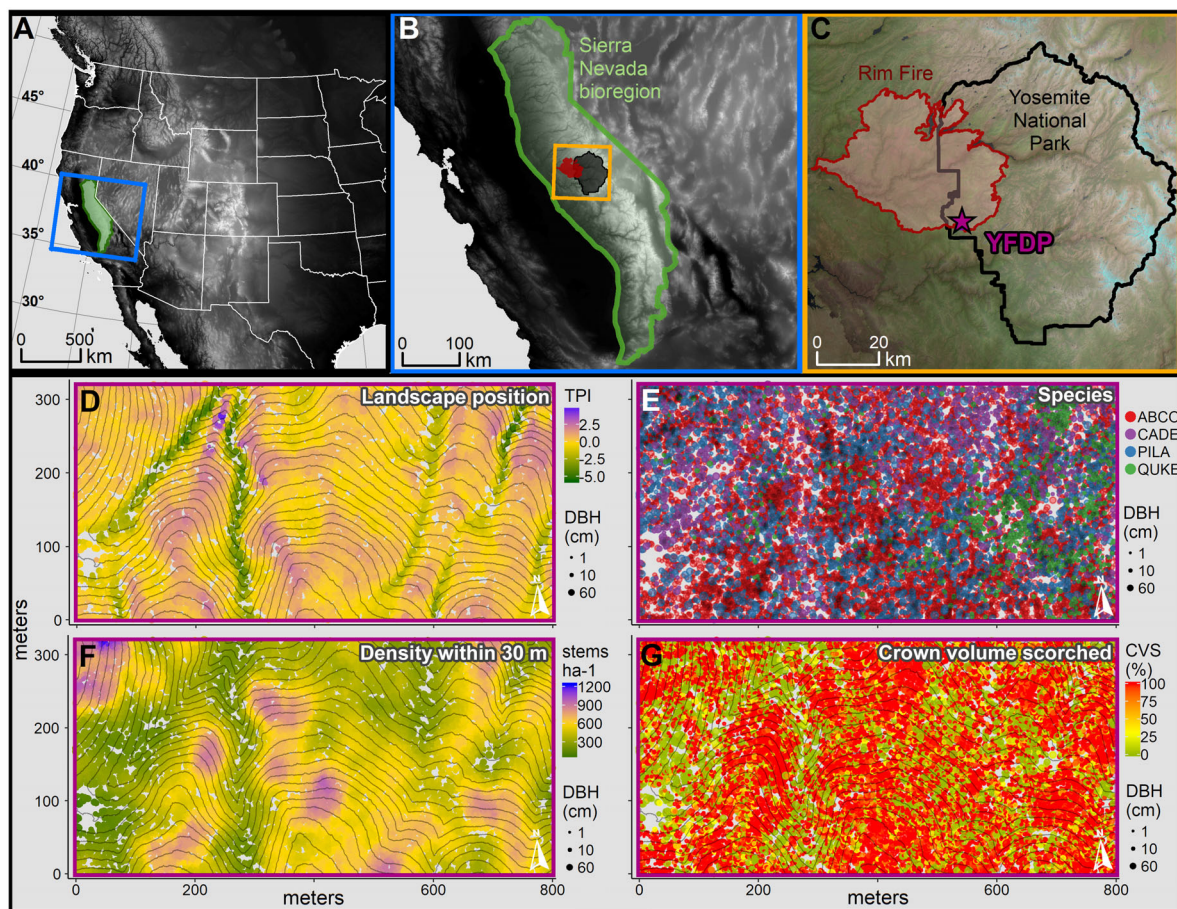


Fig. 2. Location of the Yosemite Forest Dynamics Plot (YFDP) within the lower-montane mixed-conifer zone of the Sierra Nevada, California, USA (A–C). The bottom four panels show stem maps of stems ≥ 1 cm diameter at breast height (DBH) colored according to (D) landscape position (derived from a LiDAR-measured, 1-m digital elevation model); (E) species (*Abies concolor* [ABCO], *Calocedrus decurrens* [CADE], *Pinus lambertiana* [PILA], and *Quercus kelloggii* [QUKE]); (F) neighborhood density (average density within a 30-m circular radius); and (G) crown volume scorched (CVS).

low, moderate, and high tree mortality (Furniss et al. 2020).

Pre-fire mortality was measured through annual mortality surveys in 2011, 2012, and 2013. Each year, we re-visited every tree that was alive in the previous year and we identified new mortalities (no live foliage above DBH). We conducted pathology examinations (including removing bark to inspect the cambium) on each newly dead tree and recorded the multiple factors associated with death (e.g., beetle galleries, pathogens, ruptured stem, crushing; see Appendix S1 for comprehensive list). We also recorded notes about each live tree pertaining to unique characteristics such as old fire scars. Eight months after the fire, we conducted a mortality survey to identify newly dead trees (hereafter “immediate mortality”; trees newly dead between June 2013 and May 2014). In addition to the standard pathology procedure (Appendix S1), we also recorded fire damage (bole scorch height and percent crown volume scorched; CVS) for all live and newly dead trees. Post-fire mortality was measured through annual mortality surveys for five years following the fire (hereafter “post-fire mortality”; trees that survived ≥ 1 yr post-fire but died in 2015–2018). Pathology examinations were conducted by well-trained, inter-calibrated field crews under the direct supervision of the principal investigators and experienced crew leads, with four personnel present during all ten years of measurement for continuity.

Drought during the study period.—California experienced a severe drought from 2012 to 2016 (Belmecheri et al. 2016), coinciding with two years of our pre-fire mortality surveys (2012–2013) and three years of post-fire surveys (2014–2016). We did not detect elevated mortality in the YFDP during the first two years of the drought; this is corroborated by other studies of mortality in the Sierra Nevada during these years (Byer and Jin 2017, Young et al. 2017), and it is consistent with the expectation that many trees are able to persist through the beginning of multi-year droughts (Guarín and Taylor 2005, McDowell et al. 2008). As the drought progressed, it began to cause extensive tree mortality throughout the Sierra Nevada (Young et al. 2017), peaking in severity in 2016 (Byer and Jin

2017) before subsiding following the wet winter of 2016–2017.

The timing and severity of drought-induced mortality in the Sierra Nevada are conflated with our measurements of immediate and delayed fire-related mortality. This reveals a persistent challenge regarding natural experiments in long-term monitoring plots: There is no factorial design through which treatment effects may be decoupled. Disentangling the relative contributions of drought and fire to patterns in delayed mortality is not possible with the YFDP dataset alone, and differences in sampling protocols and stand characteristics make comparisons with auxiliary datasets difficult. We note, however, that while the climatic conditions during this study were historically unprecedented (Belmecheri et al. 2016), drought and fire are expected to co-occur with increasing frequency in the coming decades (Allen et al. 2015, Berner et al. 2017); this case study may therefore provide prescient insights regarding mortality patterns following future wildfires.

Analyses

As spatially explicit mortality processes may differ among species and size classes (Das et al. 2008, Wang et al. 2012), we analyzed each species independently and grouped trees into three size classes chosen to reflect the distinct ecological roles of small (1–10 cm DBH)-, medium (10–60 cm DBH)-, and large (≥ 60 cm DBH)-diameter trees (sensu Lutz et al. 2018) while maintaining a robust sample of trees in each diameter class. We restricted all point pattern analyses to species-size classes that contained >100 individuals to minimize exposure to type II error (failure to reject the null when it is false; Rajala et al. 2018).

We grouped mortality into three regimes: pre-fire (background) mortality, direct fire-related mortality, and post-fire mortality. For each mortality regime, we assessed both the spatial structure of background mortality processes as well as the effects of local neighborhood structure on mortality risk. To characterize the spatial structure of mortality, we used two forms of point pattern analysis: the pair-correlation function (PCF) to quantitatively compare patterns, and maps of point pattern intensity to qualitatively describe, visualize, and compare patterns. To assess the

effects of forest spatial pattern on mortality risk, we used generalized linear models based on the local neighborhood spatial structure around each tree. We implemented both types of analysis for each species, size class, and mortality regime.

Point pattern analyses: pair-correlation function.— We used point pattern statistics and random labeling null models (sensu Goreaud and Pélissier 2003, Wiegand and Moloney 2004) to test whether mortality was spatially random while controlling for the underlying non-random spatial pattern of the stems within the YFDP. We summarized the observed spatial pattern of pre-fire, immediate, and post-fire mortality using the univariate form of the inhomogeneous PCF, $g(r)$, to control for underlying environmental heterogeneity and variability in first-order intensity (Wiegand and Moloney 2004). This spatial summary statistic, $g(r)$, quantifies second-order correlations between points, and this can be used to infer biological interaction between trees (Wiegand and Moloney 2004).

We compared $g(r)$ calculated for the observed pattern of mortalities to the null model of random mortality, a null model that allows one to test whether the process determining mortality is random while controlling for the underlying heterogeneous pattern of trees (Goreaud and Pélissier 2003, Wiegand and Moloney 2004). Simulations of the null model were generated by holding the observed pattern of trees constant while randomly labeling trees as mortalities in proportion to the number of actual mortalities. We selected the 25th largest and smallest values from 999 simulations to create Monte Carlo simulation envelopes around the null model with an $\alpha \sim 0.05$ (sensu Grabarnik et al. 2011, Baddeley et al. 2014). This envelope may be interpreted as the amount of variation expected if the process determining the pattern of mortality was spatially random, and deviations from the envelope indicate distances at which mortality was non-random.

We conducted a similar analysis considering only mortalities killed by bark beetles, pathogens, and physical factors (mechanical failure, crushing). Trees were grouped according to factors associated with death as recorded in the year they died (details in *Study area*). Trees that had multiple factors associated with death (e.g., both bark beetles and mechanical failure) were

included in multiple groups. We distinguished between fungal pathogens and saprophytes, and our analysis of pathogen-related mortality did not include trees that died when the stem ruptured due to saprophytic decay in the fire-killed part of the bole (these were considered mechanical mortalities). Simulations were generated by randomly selecting n trees from the superset of trees within the focal species-size class, where n is the number of mortalities associated with the focal mortality agent. We performed this analysis on pre-fire and post-fire mortality, as mortality in the year of the fire was dominated by direct fire damage.

For each mortality regime, we analyzed the trees that survived through the previous time period (i.e., direct fire mortality was assessed based on trees that were alive the year before the fire, and post-fire mortality was assessed based on trees that survived ≥ 1 yr post-fire). We conducted each analysis for all species and size classes grouped, as well as for each species-size class independently. We analyzed spatial patterns at scales ranging from 0 to 30 m because we sought to not only capture plant–plant interactions that operate at small scales (< 9 m, Das et al. 2011; < 10 m, Furniss et al. 2017; < 26.6 m, Wiegand et al. 2007), but to also capture the spatial structure of mortality associated with heterogeneous fire intensity that can occur at larger scales (Kolden et al. 2012, Larson and Churchill 2012, Yocom-Kent et al. 2015). We implemented all point pattern analyses in R v.3.5.2 (R Core Team 2018) using the package spatstat v.1.59-0 (Baddeley et al. 2015).

Point pattern analyses: maps of pattern intensity.— We created maps of mortality using the density.ppp function from the spatstat package (Baddeley et al. 2015) to estimate point pattern intensity, λ , following the methods of Diggle (1985) based on an isotropic Gaussian smoothing kernel. This spatially heterogeneous estimate of intensity provides the basis for the inhomogeneous PCF (details in Point pattern analysis: pair-correlation function), but the map of point pattern intensity itself can be used to visualize the broad-scale variability in the strength of a process (compared to the PCF which is used to assess second-order interactions at fine spatial scales; < 20 m). We repeated the random labeling procedure to create a set of simulated

realizations of mortality based on random selections of stems that were alive at the beginning of each mortality regime (i.e., simulations for post-fire mortality only included stems that survived ≥ 1 yr post-fire). For each of the 999 simulations, we created a map of point pattern intensity, and we identified the minimum and maximum expected intensity values for each 1×1 m pixel. We compared the maps of observed intensity to the range of expected values from the simulations, and we masked out areas in these observed mortality maps that were within this range. The resulting maps display heterogeneity in the intensity of mortality processes that exceeds the amount of variability that would be expected by chance.

Generalized linear models.—We summarized the structural attributes of the local neighborhood around each tree and used generalized linear models to quantify the degree to which these structural variables improved prediction accuracy compared to non-spatial null models (sensu Das et al. 2008). We quantified the importance of each structural variable by adding it as an additional independent parameter to base models which related probability of mortality to tree DBH (separate models for each structural variable). Structural variables were formulated to reflect different physical and biotic processes that may mediate fire-related mortality including competition, susceptibility to bark beetles, and pathogen activity. We calculated all structural variables for each individual tree within circular neighborhoods based on radii of 5, 10, 15, 20, and 30 m. Variables included local neighborhood basal area (BA), density of stems of each size class, nearest neighbor, and the Hegyi index (Hegyi 1974), a distance- and size-weighted competition index designed to reflect competitive inequalities related to tree size and inter-tree distance (Biging and Dobbertin 1992). We also calculated landscape position based on a 1-m LiDAR-derived digital elevation model using the methods of Wilson et al. (2007) at a scale of 53 m (scale chosen to approximate the area of a 30-m radius circle). Finally, we noted the presence of a previous fire scar by querying the field notes associated with each tree for the phrases including scar, fire scar, and cat face. For all neighborhood calculations, we corrected

for edge effects by mirroring trees within 30 m of the edge of the YFDP to create a simulated stem map buffer around the entire study area. The complete list of variables, and rationale for the formulation of each variable, may be found in Appendix S1: Table S1.

We generated separate base models for pre-fire, direct fire, and post-fire mortality. For the immediate fire mortality models, we generated two base models: one to capture the direct effects of structural variables on mortality by altering local fire intensity ($P_{\text{fire}} \sim \text{DBH}$), and one to capture the indirect effects of structural variables on immediate mortality by mediating the tree's ability to withstand fire damage. We isolated these indirect effects by including crown scorch (CVS) as an independent variable to control for the direct effects of local neighborhood on fire intensity ($P_{\text{fire}} \sim \text{DBH} \times \text{CVS}$). For the post-fire models, we included both DBH and CVS as independent variables to control for tree size and extent of fire damage ($P_{\text{post}} \sim \text{DBH} \times \text{CVS}$). Models were created using the logistic model form:

$$P = \frac{1}{1 + e^{-(\beta_0 + \beta_1 X_1 + \dots + \beta_t X_t)}}$$

where P is the probability of mortality (P_{pre} for pre-fire mortality, P_{fire} for direct fire mortality, and P_{post} for delayed), β_0 – β_t are regression coefficients, and X_1 – X_t are predictor variables (DBH, CVS, and each structural variable). We used CVS as a proxy for fire intensity because it is a tree-centric metric of fire intensity that captures the aspects of fire behavior that are most important in determining tree mortality (Sieg et al. 2006, Woolley et al. 2012, Hood and Lutes 2017). For the models that incorporated both CVS and DBH terms, we included a CVS:DBH interaction term to account for the non-linear relationship between DBH and susceptibility to CVS (Kolb et al. 2007, Furniss et al. 2019). For the delayed mortality model, we only considered trees that survived ≥ 1 yr post-fire. We compared model accuracy using Akaike's information criterion (AIC) and considered differences in AIC > 7 as support for a significant difference in model accuracy (Burnham and Anderson 1998). We did not consider any spatial variables that had a P -value > 0.01 . All analyses were performed in R ver. 3.5.2 (R Core Team 2018).

RESULTS

Pre-fire background mortality rates ranged from 0.1% to 3.2% per yr, with an overall mortality rate of 1.7% per yr considering all stems ≥ 1 cm DBH (Table 1). For *Abies* and *Calocedrus*, rates were lowest (1.4% and 0.1%, respectively) for medium-diameter trees (10–60 cm DBH), while for *Pinus*, rates were lowest (0.5%) for large-diameter stems (≥ 60 cm DBH). Pre-fire mortality rates were highest for small-diameter (1–10 cm DBH) *Abies* and *Pinus* (1.8% and 3.2%, respectively), large-diameter *Calocedrus* (0.6%), and medium-diameter *Quercus* (2.5%).

Immediate fire mortality rates were negatively related to diameter for all species, with a maximum of 95.4% (small-diameter *Pinus*) and a minimum of 2.3% (large-diameter *Pinus*; all rates may be found in Table 1). Immediate mortality was rarely attributed to factors other than fire; most trees were killed by direct fire damage alone.

Post-fire mortality rates were also greatest for small-diameter stems, with the exception of

Pinus which had the greatest mortality rate in the medium-diameter class. Post-fire mortality rates ranged from 2.7% per yr for *Calocedrus* to 22.3% per yr for small-diameter *Abies* (Table 1).

Distance-dependent mortality

Pre-fire mortality.—Pre-fire mortality was aggregated when all stems were pooled (Fig. 3), indicating the presence of distance-dependent mortality processes. Mortality was aggregated at the greatest distance for small-diameter stems (0–13 m), and this clustering of mortality was evident despite the initial pre-fire pattern of small-diameter stems also being strongly aggregated (Fig. 3; Appendix S1: Fig. S1). Pre-fire mortality of medium-diameter stems was similarly aggregated, but the clustering of mortality was more clearly differentiated because the initial pattern of medium-diameter stems was more regular (i.e., less aggregated) compared to the initial pattern of small-diameter stems (Fig. 3). The spatial pattern of large-diameter mortalities was generally random, but this randomness may indicate a slightly clustered pattern of mortality

Table 1. Pre-fire mortality, direct fire mortality, and post-fire mortality for trees within the Yosemite Forest Dynamics Plot.

			Number of mortalities														
			Pre-fire					Direct fire (<1 yr)					Post-fire				
DBH (cm)	N live at est.	N live at end	Beet.	Path.	Mech.	Total	Rate (% yr ⁻¹)	Beet.	Path.	Mech.	Total	Rate (% yr ⁻¹)	Beet.	Path.	Mech.	Total	Rate (% yr ⁻¹)
<i>Abies</i>																	
1–10	15,001	375	240	149	266	790	1.8	5	28	91	13,183	92.8	124	66	37	653	22.3
10–60	9630	2268	258	97	115	406	1.4	16	104	51	4183	45.3	778	743	304	2773	18.1
≥60	597	421	11	6	2	27	1.5	3	3	3	22	3.9	33	41	8	127	6.4
<i>Calocedrus</i>																	
1–10	936	76	1	5	9	15	0.5	0	0	10	799	86.8	9	1	1	46	11.2
10–60	608	294	0	0	0	1	0.1	0	1	11	234	38.6	4	7	10	79	5.8
≥60	107	85	0	0	1	2	0.6	0	2	1	10	9.5	0	1	3	10	2.7
<i>Pinus</i>																	
1–10	2705	71	89	48	69	251	3.2	1	4	18	2342	95.4	13	2	3	41	10.8
10–60	1532	399	40	17	24	64	1.4	36	24	8	581	39.6	289	61	17	488	18.1
≥60	706	402	4	3	6	10	0.5	7	5	3	16	2.3	250	22	9	278	12.3
<i>Quercus</i>																	
1–10	426	37	2	2	11	27	2.2	0	1	11	332	83.2	0	0	3	30	13.8
10–60	740	249	9	4	6	55	2.5	0	0	11	348	50.8	0	5	9	88	7.3
≥60	1	1	0	0	0	0	...	0	0	0	0	...	0	0	0	0	...

Notes: “...” stands for NA. Values represent the number of mortalities associated with bark beetles (Beet.), pathogens (Path.), and mechanical (Mech.; e.g., broken stem or crushed) factors associated with death. Individual trees may be associated with multiple factors. Columns reflect the number of mortalities associated with bark beetles, pathogens, and mechanical agents of mortality, while Rate (% per yr) reflects annualized mortality rates. Bold indicates categories with enough stems to be used in spatial analysis ($n > 100$).

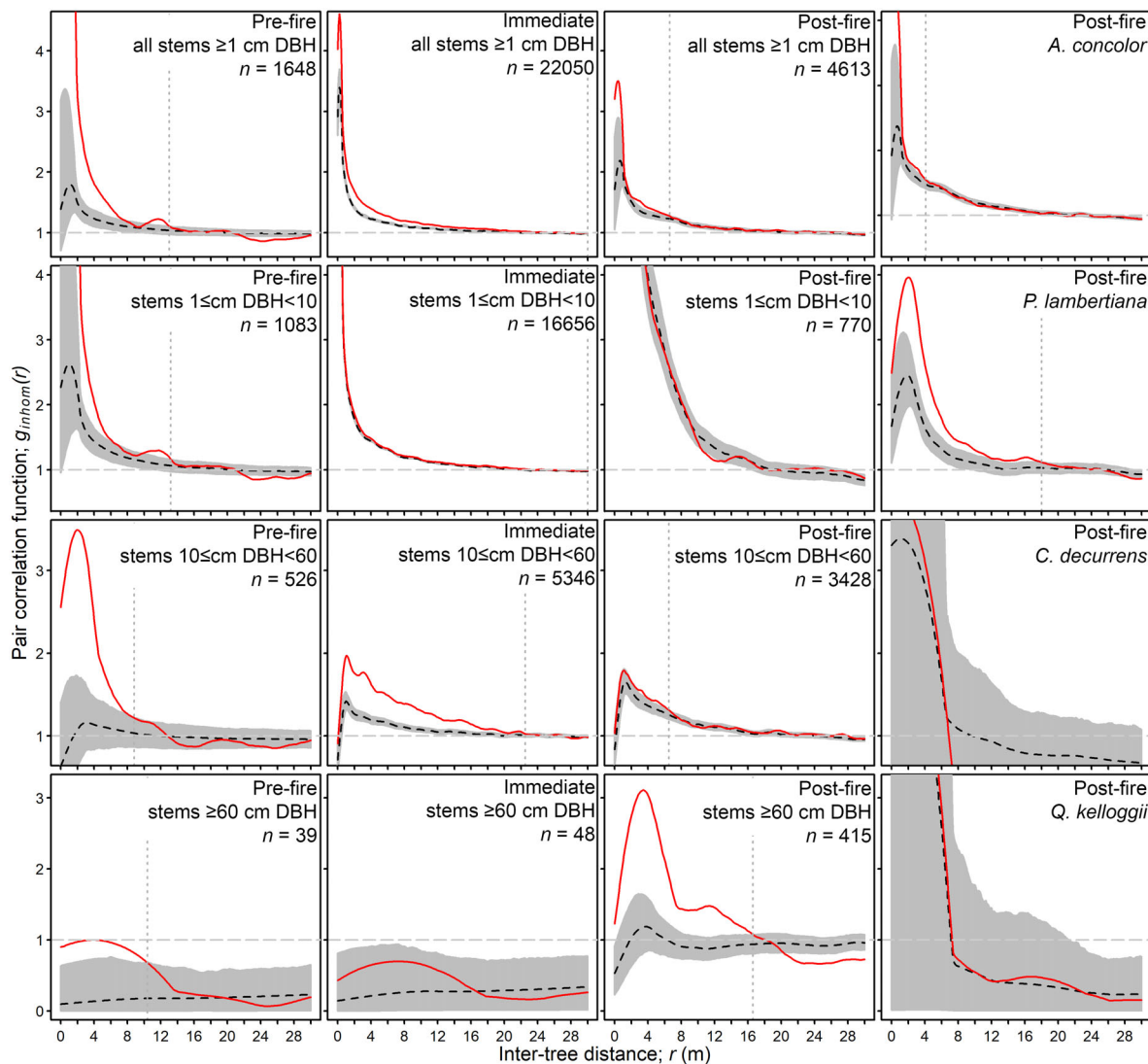


Fig. 3. Spatial pattern of pre-fire mortality, direct fire mortality, and post-fire mortality within the Yosemite Forest Dynamics Plot. The red lines indicate observed patterns, shaded areas represent Monte Carlo simulation envelopes based on the 2.5th and 97.5th percentiles of 999 simulations generated according to the null hypothesis of random mortality, and dashed lines represent the mean value of simulations. Black dashed lines represent the mean value from the simulations. Vertical dotted lines represent the distance (r) at which the observed pattern of mortality became random. Values of $g(r)$ above the shaded envelope indicate that mortality was aggregated, while values below the envelope indicate hyper-dispersed mortality.

because the initial pattern of large-diameter trees was hyper-dispersed (Appendix S1: Fig. S1).

Mortality associated with bark beetles was aggregated for all species-size classes (Fig. 4; n for each indicated by bold in Table 1). Beetle-related mortality was aggregated from 0 to 4 m for

small-diameter (1–10 cm DBH) *Abies*, from 0 to 6 m for medium-diameter *Abies*, and from 0 to 10 m for *Pinus* of all sizes (Fig. 4). Mechanical mortality was also aggregated for small- and medium-diameter *Abies* from 0 to 6 m and 10 to 22 m, respectively. Pathogen mortality was

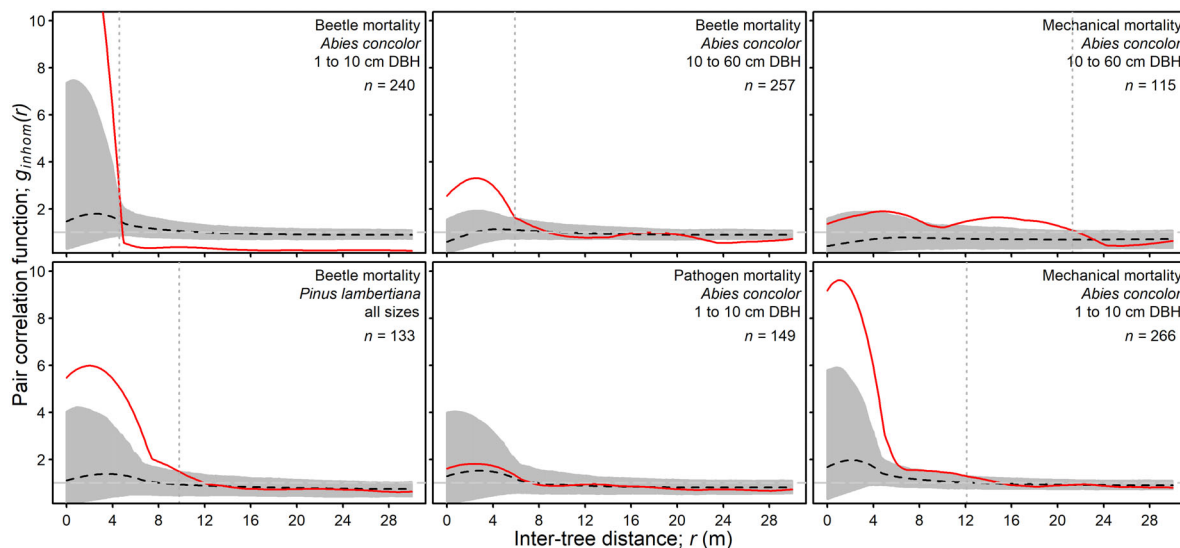


Fig. 4. Spatial pattern of agent-specific pre-fire mortality within the Yosemite Forest Dynamics Plot. The red lines indicate observed patterns, shaded areas represent Monte Carlo simulation envelopes based on the 2.5th and 97.5th percentiles of 999 simulations generated according to the null hypothesis of random mortality, and dashed lines represent the mean value of simulations. The vertical dotted lines represent the distance (r) at which the observed pattern of mortality became indistinguishable from the null model; values of $g(r)$ above the shaded envelope indicate clustered mortality while values below indicate hyper-dispersed mortality. Sample size, n , is the number of points in each pattern.

spatially random for small-diameter *Abies*, the only size class that had sufficient numbers of mortality to test (Fig. 4).

Direct fire mortality.—Immediate fire mortality was strongly aggregated for all stems grouped from 0 to 30 m (Fig. 3). Fire-induced mortality of small-diameter stems alone was also aggregated from 0 to 30 m, while mortality of medium-diameter stems was aggregated from 0 to 23 m (Fig. 3). Large-diameter mortality appeared random (Fig. 3), though the immediate mortality rate of large-diameter stems was very low (Table 1).

Post-fire mortality.—Post-fire mortality of all stems ≥ 1 cm DBH was aggregated from 0 to 7 m, a finer scale compared to both pre-fire and direct fire mortality (Fig. 3). Post-fire mortality of small stems was random, while medium-diameter mortalities were slightly aggregated from 0 to 8 m (Fig. 3). Post-fire mortality of large-diameter trees, in contrast, was strongly clustered and at greater scales compared to pre-fire mortality (0–17 m; Fig. 3). The emergence of strongly clustered large-diameter tree mortality was readily

apparent in the field and is also visually discernable from the stem maps of mortality (Appendix S1: Fig. S1). Considering species individually, post-fire mortality was aggregated from 0 to 4 m for *Abies*, from 0 to 17 m for *Pinus*, and was spatially random for *Calocedrus* and *Quercus* (Fig. 3).

Post-fire mortality was mediated by biotic and mechanical mortality processes that were spatially structured for all species and diameter classes that we tested. Bark beetle mortality was aggregated for medium-diameter *Pinus* from 0 to 12 m, large-diameter *Pinus* from 0 to 18 m, and medium-diameter *Abies* from 1 to 8 m (Fig. 5). Mechanical mortality was aggregated for medium-diameter *Abies* from 0 to 5 m and 16 to 19 m. Pathogen mortality was also aggregated for medium-diameter *Abies* from 2 to 3.5 m (Fig. 5).

Geographic patterns in mortality

Pre-fire mortality.—Maps of mortality intensity revealed complex patterns of mortality across the YFDP. Pre-fire mortality of small- and medium-

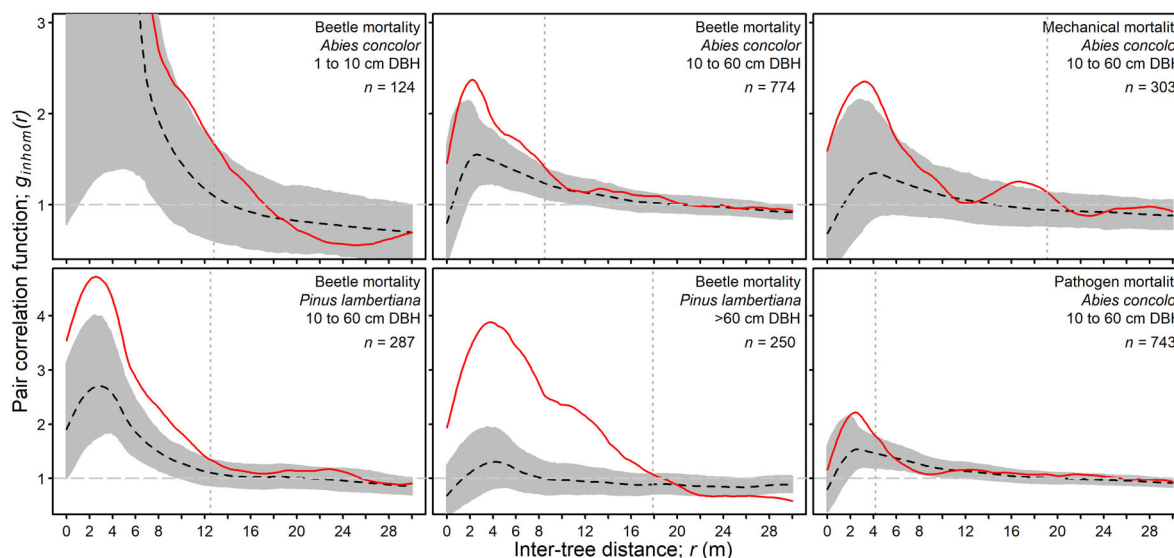


Fig. 5. Spatial pattern of agent-specific post-fire mortality within the Yosemite Forest Dynamics Plot. The red lines indicate observed patterns, shaded areas represent Monte Carlo simulation envelopes based on the 2.5th and 97.5th percentiles of 999 simulations generated according to the null hypothesis of random mortality, and dashed lines represent the mean value of simulations. The vertical dotted lines represent the distance (r) at which the observed pattern of mortality became indistinguishable from the null model; values of $g(r)$ above the shaded envelope indicate clustered mortality while values below indicate hyper-dispersed mortality. Sample size, n , is the number of points in each pattern.

diameter stems was characterized by patches of both high and low mortality rates separated by regions of random, ambient mortality (Fig. 6; Appendix S1: Fig. S1). The spatial distribution of pre-fire large-diameter mortalities, however, was random.

Direct fire mortality.—Direct fire mortality for all size classes exhibited a stronger spatial structure, with larger patches of both elevated and reduced mortality intensity and more area overall that was characterized as non-random. The patches of non-random pre-fire mortality did not simply expand to accommodate the greater number of direct fire mortalities; the distribution of non-random immediate fire mortality assumed a distinct geography (Fig. 6). Many areas that were characterized by random mortality pre-fire assumed a non-random spatial structure due to direct fire mortality (e.g., southeast corner of the YFDP in Fig. 6). This pattern likely reflected the spatial heterogeneity in pre-fire fuel loadings that caused variability in first-order fire intensity and concomitant mortality across the YFDP (Blomdahl et al. 2019, Cansler et al. 2019, Furniss et al.

2020). As with the pre-fire regime, large-diameter mortality was still mostly random, but the direct fire effects did create two small patches of non-random mortality in this size class.

Post-fire mortality.—The pattern of post-fire mortality assumed a yet third distinct distribution and did not resemble the patterns of either pre-fire or direct fire mortality (Fig. 6; Appendix S1: Fig. S1). For small- and medium-diameter stems, the area characterized by random mortality increased slightly compared to direct fire mortality, but for medium-diameter stems the total area of non-random mortality was still greater than during the pre-fire regime. In contrast, post-fire mortality of large-diameter trees developed strong spatial structure that was absent during both pre- and direct fire mortality regimes. Some of these patches of non-random large-diameter mortality overlapped with areas of non-random medium-diameter mortality, but some patches were unique. For example, we observed elevated large-diameter mortality in the northwest part of the YFDP, but the mortality rate of medium-diameter trees in this same area

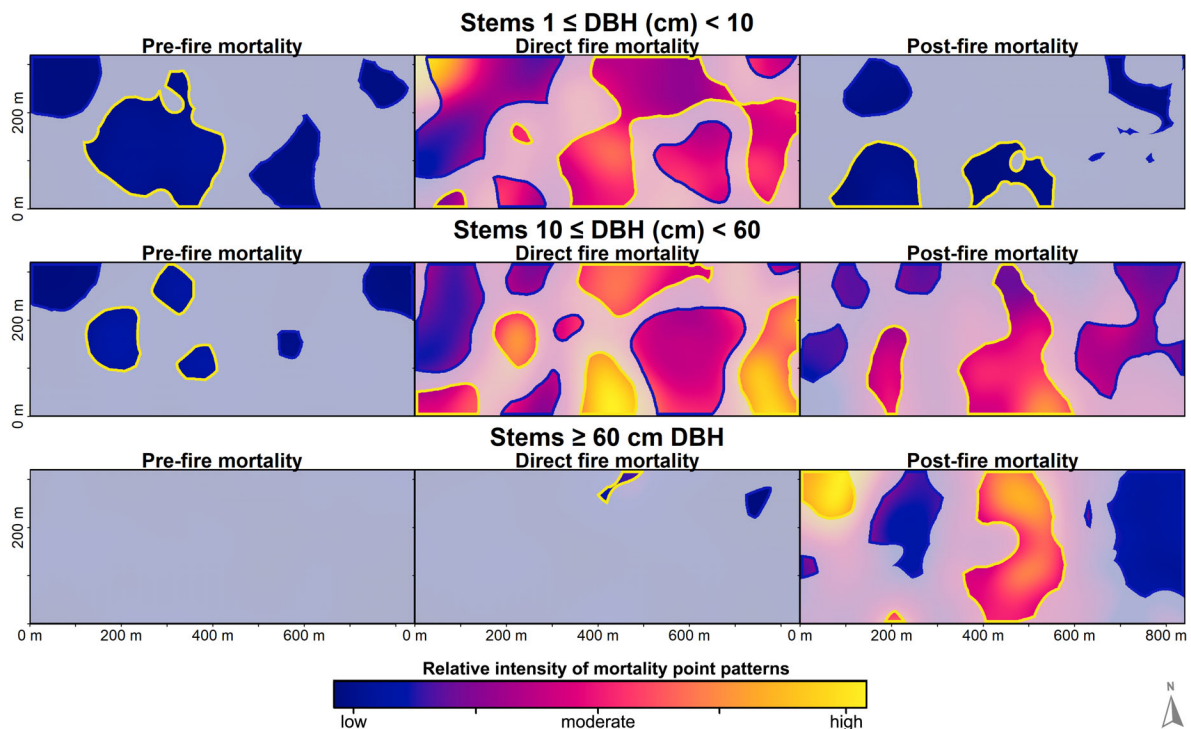


Fig. 6. Maps of mortality intensity (kernel density estimation) of pre-fire, direct fire, and post-fire tree mortality within the Yosemite Forest Dynamics Plot. Colors are relativized per tree diameter class (i.e., yellow for small-diameter trees represents a higher absolute rate compared to yellow for large-diameter trees; Table 1 contains absolute mortality rates). Line color around each polygon indicates whether mortality was higher or lower than would be expected by chance based on the non-random initial pattern of live stems at the beginning of each mortality regime (blue indicates reduced mortality rates; yellow indicates elevated mortality rates). For example, a yellow line around a blue polygon represents a low relative mortality rate (blue fill) that was still higher than would have been expected by chance (yellow border line). The pattern of stems associated with each panel may be found in Appendix S1: Fig. S1.

was lower than would have been expected by chance (Fig. 6).

Density-dependent mortality

Pre-fire mortality.—Spatial variables improved predictions of pre-fire mortality for small- and medium-diameter *Abies*, medium-diameter *Pinus*, and *Quercus* ≥ 10 cm DBH (Table 2; Appendix S1: Table S2). Density of pole-sized conspecifics was the single most important variable in most cases, while BA was more important for *Abies*. The direction of the relationship was not consistent; density increased probability of mortality for small-diameter *Abies*, while density decreased probability of mortality for medium-diameter *Pinus* and *Quercus* (Figs. 7, 8;

Appendix S1: Fig. S2). Pre-fire mortality of large-diameter trees was density-independent for the three conifer species (Figs. 7–9).

Direct fire mortality.—Structural variables improved mortality model accuracy for both immediate and delayed fire-related mortality for all species (Table 2, Figs. 7–9; Appendix S1: Fig. S2 and Table S3). Structural variables enhanced the immediate-direct models (did not include CVS) for small- and medium-diameter trees of all species, and structural variables improved the immediate-indirect models (did include CVS) for small *Pinus*, all *Quercus*, and medium *Calocedrus*. Local neighborhood density and BA were positively related to both immediate and delayed mortality for most species-size

Table 2. Mortality rates and spatial metrics that were correlated with mortality.

DBH (cm)	Important structural variables					
	Pre-fire	Δ AIC	Direct fire	Δ AIC C	Post-fire	Δ AIC
<i>Abies</i>						
1–10	Density of conspecifics ≥ 10 cm DBH (10 m) (+)	–92.7	Density of conspecifics ≥ 10 cm DBH (30 m) (+)	–177.4	BA (5 m) (+)	–48.9
10–60	BA (30 m) (–)	–33.0	BA of conspecifics (30 m) (+)	–99.6	Density surviving stems $1 \leq$ cm DBH < 10 (10 m) (–)	–125.9
≥ 60	Density of stems $10 \leq$ cm DBH < 60 (10 m) (–)	–5.4	Density of conspecifics ≥ 10 cm DBH (30 m) (+)	–6.3	Density of stems ≥ 60 cm DBH (20 m) (+)	–15.2
<i>Calocedrus</i>						
1–10	Density of all stems ≥ 1 cm DBH (20 m) (–)	–5.6	Landscape position (+)	–38.5	BA surviving conspecifics (20 m) (+)	–13.9
10–60	Density of all stems ≥ 1 cm DBH (30 m) (–)	–3.0	BA of conspecifics ≥ 10 cm DBH (30 m) (–)	–12.6	BA surviving conspecifics (5 m) (+)	–7.8
≥ 60	Density of stems $10 \leq$ cm DBH < 60 (30 m) (+)	–1.9	BA (30 m) (–)	–5.8	BA (30 m) (+)	–2.8
<i>Pinus</i>						
1–10	Hegyi (+)	–3.9	BA (5 m) (+)	–22.1	BA surviving conspecifics (30 m) (+)	–4.8
10–60	Density of conspecifics ≥ 10 cm DBH (20 m) (–)	–9.8	Density of stems ≥ 1 cm DBH (5 m) (–)	–9.8	BA of conspecifics ≥ 10 cm DBH (10 m) (+)	–37.2
≥ 60	BA of conspecifics ≥ 10 cm DBH (10 m) (–)	–6.2	Fire scar (+)	–24.0	Hegyi (+)	–76.8
<i>Quercus</i>						
1–10	Nearest neighbor (+)	–4.6	Density of stems $10 \leq$ cm DBH < 60 (15 m) (+)	–41.4	...	
≥ 10	Density of conspecifics ≥ 10 cm DBH (10 m) (–)	–22.9	Hegyi (+)	–41.6	BA (30 m) (+)	–13.7

Notes: BA, basal area; CVS, crown volume scorched; DBH, diameter at breast height. “...” stands for, no variables were significant. Correlations were identified by pairing each variable with non-spatial base models based on DBH and CVS. This table contains the single best structural variable for each species and size class; all significant variables are reported in Appendix S1: Tables S2–S4. Descriptions of each variable are in Appendix S1: Table S1. The distance values each variable indicate the circular radius at which that structural variable had the most explanatory power. The (+) or (–) next to the structural variable indicates the direction of the relationship (positive indicates greater mortality risk; negative indicates lower mortality risk). Delta Akaike information criterion (Δ AIC) represents the differential model performance compared to the base (non-spatial) mortality models; more negative numbers indicate greater improvement. Bold indicates that the spatial model was significantly better than the non-spatial base model ($|\Delta$ AIC| > 7).

classes (Table 2; Appendix S1: Table S3). Density and BA of conspecifics within 30 m were the most important structural variables for immediate mortality of small- and medium-diameter *Abies*, respectively (Fig. 7). Landscape position was the best predictor of immediate mortality for small- and medium-diameter *Calocedrus* (Table 2); mortality of small-diameter *Calocedrus* was related to the landscape position variable directly (higher mortality in xeric areas), while mortality of medium-diameter *Calocedrus* was evident in the negative association between mortality risk and conspecific BA (*Calocedrus* BA is

higher in mesic areas [negative TPI] in Fig. 2D). Immediate mortality of small-diameter *Pinus* was positively related to local neighborhood BA and density, but the presence of a fire scar was the best predictor of immediate mortality for medium- and large-diameter *Pinus*. Direct and indirect immediate mortality of *Quercus* was strongly related to local neighborhood density and the Hegyi index (Table 2; Appendix S1: Fig. S2 and Table S3).

Post-fire mortality.—Post-fire mortality models were improved by structural variables, especially for medium- and large-diameter trees (Figs. 7–9,

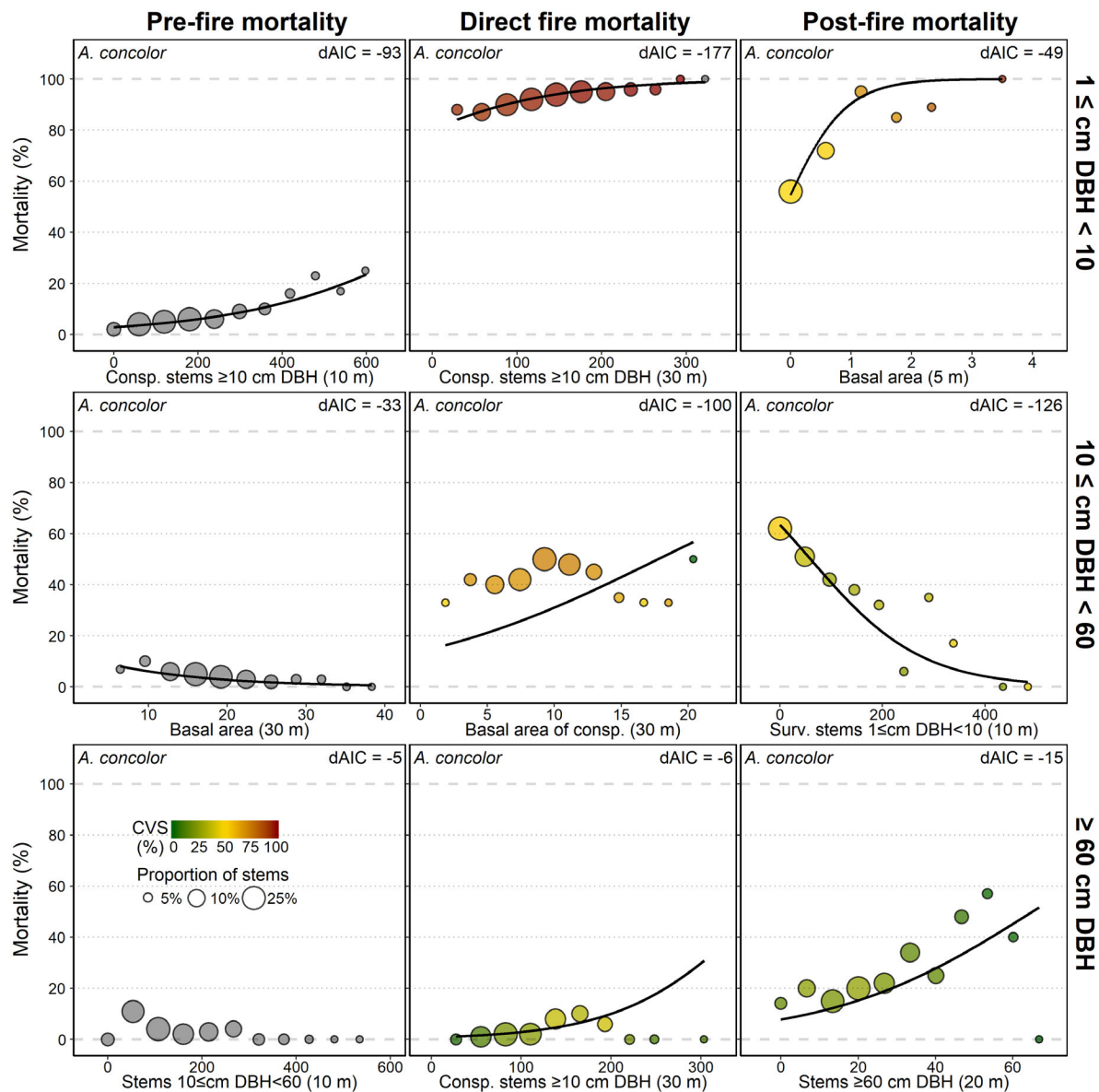


Fig. 7. Relationships between forest spatial structure and *Abies concolor* mortality. Columns represent timing of mortality, and rows represent tree diameter classes. Lines show the relationship between forest spatial structure and probability of mortality determined with generalized linear models. Points indicate observed proportion of mortality, and point size reflects relative number of stems in each group. The x-axis for each panel shows the single best structural variable for that mortality regime and size class; all variables may be found in Appendix S1: Tables S2–S4. dAIC indicates the improvement in model accuracy compared to AIC of the non-spatial base model. Basal area is reported in m²/ha, and stem categories are in stems/ha.

Table 2; Appendix S1: Table S4). A greater number of structural variables were correlated with post-fire mortality compared to either pre-fire or direct fire mortality for all three conifers

(Appendix S1: Tables S2–S4). For medium- and large-diameter *Abies* and *Pinus*, spatial variables improved model AIC for post-fire models more than they did for either pre- or direct fire models

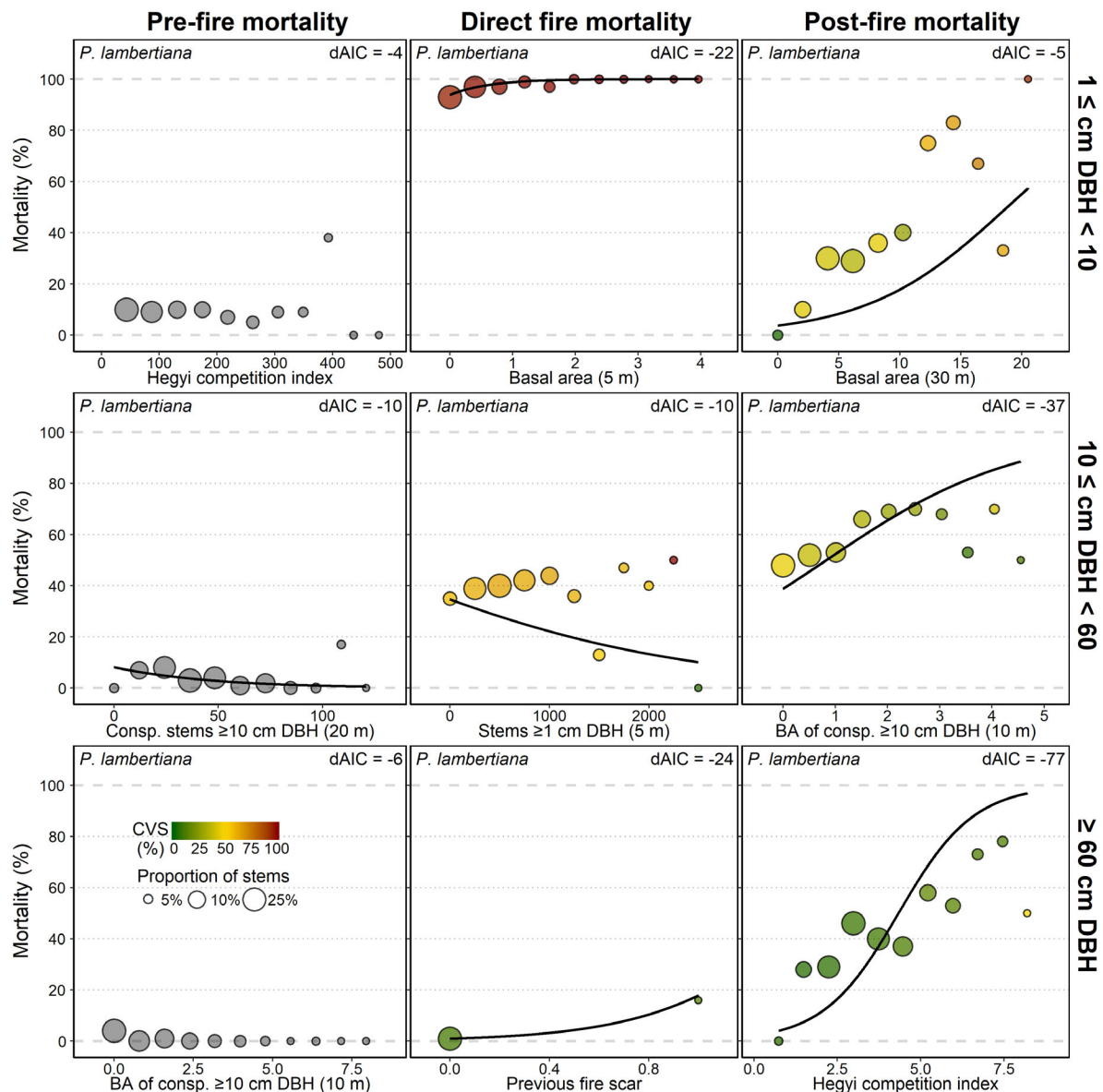


Fig. 8. Relationships between forest spatial structure and *Pinus lambertiana* mortality. Columns represent timing of mortality, and rows represent tree diameter classes. Lines show the relationship between forest spatial structure and probability of mortality determined with generalized linear models. Points indicate observed proportion of mortality, and point size reflects relative number of stems in each group. The x-axis for each panel shows the single best structural variable for that mortality regime and size class; all variables may be found in Appendix S1: Tables S2–S4. dAIC indicates the improvement in model accuracy compared to AIC of the non-spatial base model. Basal area (BA) is reported in m²/ha, and stem categories are in stems/ha.

(Table 2). Probability of delayed mortality was positively related to local neighborhood density and BA, with the exception of medium-diameter *Abies* which was negatively related to density of

surviving small-diameter stems within 10 m (Fig. 7). Species identity of neighboring stems was important for *Calocedrus* and *Pinus*; delayed mortality of both species was positively related

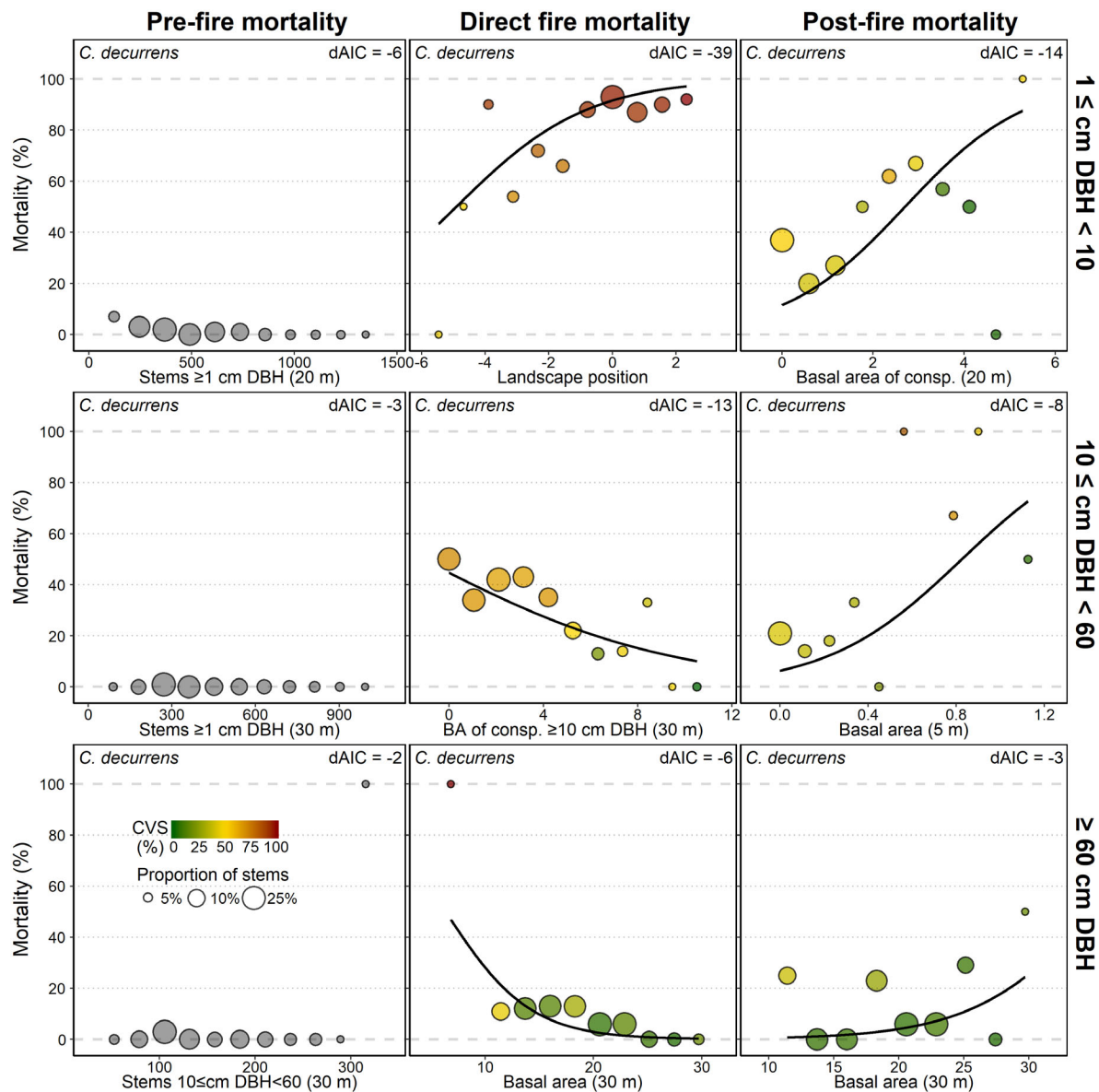


Fig. 9. Relationships between forest spatial structure and *Calocedrus decurrens* mortality. Columns represent timing of mortality, and rows represent tree diameter classes. Lines show the relationship between forest spatial structure and probability of mortality determined with generalized linear models. Points indicate observed proportion of mortality, and point size reflects relative number of stems in each group. The x-axis for each panel shows the single best structural variable for that mortality regime and size class; all variables may be found in Appendix S1: Tables S2–S4. dAIC indicates the improvement in model accuracy compared to AIC of the non-spatial base model. Basal area (BA) is reported in m^2/ha , and stem categories are in stems/ha.

to BA of conspecifics (Figs. 8, 9). The Hegyi competition index was the best local neighborhood variable for delayed mortality of large-diameter *Pinus*, but first-order structural metrics (BA and

density) were better predictors for other species-size classes (Table 2). Neither density of previous year beetle-related mortality nor density of previous year pathogen-related mortality were

significant predictors of delayed mortality for any species.

DISCUSSION

Fire is an important driver of spatial pattern dynamics (Larson and Churchill 2012), but ecological factors that mediate delayed mortality including climate, bark beetles, and competition (van Mantgem et al. 2013, 2018, Hood et al. 2018) have distinct spatial signatures (Fig. 1) that may contribute to emergent patterns in mortality. These delayed mortality processes are particularly important for fire-tolerant species and large-diameter trees, as these trees are able to withstand the damage associated with low- and moderate-severity fire alone. This study demonstrates that the interactive effects of compound disturbances (fire and drought) and background mortality processes can transform the spatial elements of mortality by altering the scale of distance-dependent processes, increasing the intensity of density dependence, and provoking spatially non-random mortality among large-diameter trees.

The results of this study support our second alternative hypothesis that background mortality processes interact with acute disturbances to create a novel mortality regime. Before fire, density-dependent mortality was only evident among the smallest trees, but the combined effects of fire, drought, and background mortality processes provoked density-dependent mortality among medium- and large-diameter trees as well. Immediate fire effects extended the spatial scale of distance-dependent mortality, and post-fire mortality of large-diameter trees became strongly aggregated. The intensity of mortality assumed a unique spatial distribution throughout the study site, and patches of elevated mortality emerged where they were not present before. The compound effects of fire, drought, and background mortality processes altered both distance- and density-dependent mortality mechanisms, creating a post-fire mortality regime with a more complex spatial structure compared to either pre-fire mortality or direct fire damage. While immediate fire effects were highly conspicuous, the majority of mortality was among small-diameter stems and the spatial structure was driven primarily by variation in fire

intensity. The more ecologically consequential effects of fire were heavily influenced by the interactive effects of severe drought and biotic mortality agents (i.e., bark beetles) that mediated a period of spatially complex mortality among large and old trees that will have enduring impact on the spatial pattern of this forest.

Pre-fire mortality

The overall pre-fire mortality rate of 1.7% per yr was within the range of variability expected based on other long-term forest demography plots in similar forest types within the Sierra Nevada (1.5% per yr; Stephenson and van Mantgem 2005). Sample size constraints limited our assessment of pre-fire mortality for some agents, underscoring the difficulties associated with detecting slow-acting ecological processes such as tree mortality, even within large forest monitoring plots (Clark and Clark 1996, Lutz 2015, Das et al. 2016, Birch et al. 2019a, McMahon et al. 2019b).

Pre-fire mortality was aggregated at fine spatial scales (0–13 m considering all stems; Fig. 3), a pattern of mortality observed in both young and old forests (Kenkel 1988, Das et al. 2008, Lutz et al. 2014, Larson et al. 2015, Furniss et al. 2017). This scale of interaction is consistent with (although slightly larger than) previous studies that have quantified the scale at which second-order (i.e., plant–plant) interactions can moderate mortality risk (4.5 m in Kenkel 1988, 5 m in He and Duncan 2000, 3 m in Little 2002, 4 m in Yu et al. 2009, 9 m in Das et al. 2011, 9 m in Lutz et al. 2014, 4 m in Larson et al. 2015, 10 m in Punchi-Manage et al. 2015, 6 m in Clyatt et al. 2016, 3 m in Furniss et al. 2017, 5 m in Birch et al. 2019b).

Mortality was clustered for stems of all sizes, but strength and directionality of density dependence varied depending on tree species and size class (Figs. 7–9). Pre-fire mortality of small *Abies* stems was positively related to neighborhood density of conspecifics (i.e., negative density dependence), while mortality risk of medium-diameter *Abies*, *Pinus*, and *Quercus* was negatively related to BA and conspecific density (i.e., positive density dependence; Figs. 7, 8; Appendix S1: Fig. S2). These opposing forms of density dependence reflect the importance of competition as a primary determinant of mortality for small-

diameter trees (Das et al. 2008, 2011, Lutz et al. 2014), and the importance of external factors (i.e., pests, pathogens, and physical damage) that compose the mortality complexes responsible for medium- and large-diameter tree mortality (Franklin et al. 1987, Das et al. 2011, 2016). These results are consistent with the expectation that background mortality transitions from strongly density-dependent within young forests to density-independent among mature trees in old-growth forests (He and Duncan 2000, Gray and He 2009, Yu et al. 2009, Aakala et al. 2012, Hurst et al. 2012, Johnson et al. 2014, Larson et al. 2015), and they provide a more nuanced understanding of this transition by demonstrating that density dependence can continue to regulate mortality among small-diameter stems even within a structurally complex, old-growth forest.

A likely source of the competitive stress responsible for the density-dependent mortality of small-diameter *Abies* is intraspecific competition from other small-diameter *Abies*. These stems were strongly aggregated (Fig. 3; Lutz et al. 2012) and were most abundant in areas with high conspecific density (>1000 stems/ha; Figs. 2, 7), and we may therefore expect mortality in these sites to resemble the self-thinning characteristic of dense, young forests (Kenkel 1988, Gray and He 2009, Larson et al. 2015). Another likely source of competitive stress is strong asymmetric competition from larger trees; the physical dominance of large trees provides them with superior access to both above- and below-ground resources, and this can inhibit survival of smaller trees within their local neighborhood (Lutz et al. 2014, Furniss et al. 2017).

There are a few plausible reasons for the positive density dependence we observed among medium-diameter trees (mortality risk decreased with greater BA and conspecific density; Figs. 7, 8; Appendix S1: Fig. S2). First, the local neighborhoods around medium-diameter trees were characterized by lower densities (up to 200 stems/ha; Fig. 8; Appendix S1: Fig. S2) and more regular spacing (Fig. 3; Lutz et al. 2012) compared to small-diameter trees. The reduced crowding in these more open neighborhoods may have reduced overall competitive stress, but this does not fully explain the reversed directionality of density dependence. Second, this pattern of positive density dependence may be associated with

environmental heterogeneity within the YFDP. We would expect medium-diameter trees to be most abundant in high-quality habitats within the YFDP (i.e., environmental filtering; Das et al. 2018), and we might also expect mortality rates to be lowest in these favorable sites; the combination of these two factors could elicit a pattern of positive density dependence. Finally, below-ground fungal symbionts (i.e., ectomycorrhizae; Perry et al. 1989) can confer facilitative effects that may have contributed to this pattern.

These results provide two interesting contrasts with a previous study from similar forests in the Sierra Nevada (Das et al. 2008). First, the authors observed CNDD (i.e., mortality risk increased with higher conspecific density) for *P. lambertiana* ≥ 12.7 cm DBH, while we found that mortality risk decreased with increasing conspecific BA for stems 10–60 cm DBH for that species (Fig. 8). Second, they observed a pattern of positive conspecific density dependence for *A. concolor* (of all sizes); our results were consistent with this for medium-diameter stems, but we observed the opposite pattern among small-diameter stems. These contrasts demonstrate that while local neighborhood structure and composition are important factors determining mortality risk, the nature of neighborhood effects may vary among forest stands. Additionally, grouping trees by diameter may have enabled us to detect neighborhood effects that may be neutralized if all sizes are analyzed together.

Spatial patterns of mortality were also driven by the distance-dependent nature of pests, pathogens, and physical damage, and each of these mortality processes had a distinct spatial structure. Bark beetle-induced mortality of small- and medium-diameter *Abies* was aggregated at very fine scales (0–6 m; Fig. 4), while beetle mortality for *Pinus* was aggregated to slightly larger scales (0–10 m). Mechanical mortality (i.e., crushing) was aggregated at the greatest scales for small- and medium-diameter *Abies* (0–12 m and 0–21 m, respectively; Fig. 4). This is consistent with our a priori conceptualization of these two mortality agents—both bark beetle and mechanical mortality are aggregated at very fine scales (<0.1 ha), but we expected mechanical mortality to remain aggregated at slightly larger scales due to the large height (up to 55 m) and potential propagation of large falling trees (Fig. 1A).

We did not detect a spatial structure associated with pathogen-related mortality, perhaps because the slow rate of pathogen spread may necessitate a longer time span for their spatial structure to be detected (Waring et al. 1987, Lung-Escarmant and Guyon 2004). Additionally, our analysis of pre-fire pathogen mortality was limited to small-diameter *Abies* (due to sample size constraints) and competition was a more important driver of mortality for small stems.

Although previous studies have quantified the spatial structure associated with these mortality agents independently (Safranyik and Carroll 2006, Das et al. 2008, Larson and Franklin 2010, Bače et al. 2015, Fig. 1A), this study is the first that we are aware of that has quantitatively compared the spatially contagious nature of endemic bark beetle mortality, pathogens, and mechanical-related tree mortality within the same study site.

Direct fire mortality

Immediate fire mortality was aggregated for small- to medium-diameter stems from 0 to 30 and 0 to 22 m, respectively (Fig. 3). This was likely driven primarily by heterogeneity in fuel loadings (Cansler et al. 2019) and topography (Fig. 2) that altered fire behavior and resulted in patches of high and low crown scorch across the YFDP (Fig. 2). Crown scorch was the strongest predictor of immediate mortality (Furniss et al. 2019), causing the spatial structure of immediate mortality to closely reflect the heterogeneity in fire intensity and flame length (Figs. 2g, 6). The spatial structure of immediate mortality was clustered at the greatest inter-tree distance of any form of mortality that we assessed (30 m; Fig. 3), distinguishing direct fire mortality as a key driver of structural heterogeneity and spatial pattern at slightly broader spatial scales (0.1–1 ha) compared to background mortality (Fig. 1).

Local neighborhood structure was directly related to probability of immediate mortality, presumably because higher stem density was associated with increased fuel loadings (Cansler et al. 2019) that elevated fire intensity (Miller and Urban 1999b, Thaxton and Platt 2006) and induced greater damage to trees. Surprisingly, forest structure was also related to probability of direct fire mortality when we included crown

scorch as a predictor variable to control for variability in fire intensity (Table 2), suggesting that forest spatial structure also influenced probability of direct mortality by reducing tolerance of individual trees to direct fire damage (perhaps by modifying local water availability and competitive stress; van Mantgem et al. 2018).

Local neighborhood structure was not of equal importance for all trees; landscape position was more important for immediate mortality of small- to medium-diameter *Calocedrus*, and the presence of a previous fire scar the most important factor for immediate mortality of medium- to large-diameter *Pinus*. The importance of fire scars for *Pinus* mortality reflects their tolerance to direct fire damage due to thick bark and high crown base heights, making them less exposed to heat-induced injury (Hood et al. 2018), yet uniquely susceptible to physical failure at scars incurred from past fire events (Kolb et al. 2007, Furniss et al. 2019).

Our findings reveal an important disparity between the scales at which fire operates and the scales at which fire effects are most often monitored. Fire creates ecological mosaics at intermediate and broad scales (>1 ha; Turner et al. 1997, Hessburg et al. 2005, Yocom-Kent et al. 2015, Meddens et al. 2018a), but fine-scale (0.1–1 ha) heterogeneity in fire effects performs distinct, and similarly important, ecological functions (Meddens et al. 2018b). Low-, moderate-, and mixed-severity fire introduces spatial pattern complexity (Larson and Churchill 2012, Churchill et al. 2013, Kane et al. 2013, 2014), mitigates susceptibility to drought, competition, and beetle-related mortality (Kolb et al. 2007, Hood et al. 2015, 2016, van Mantgem et al. 2016), and confers resilience to future disturbances and climatic variability (Allen et al. 2002, Hessburg et al. 2015, Cansler et al. 2018, Stephens et al. 2018, North et al. 2019). Fine-scale heterogeneity in fire effects is an essential component of these ecological functions, yet a vast amount of fire science is based on remotely sensed severity products that are limited to the relatively coarse spatial resolution of hyperspectral satellite sensors (e.g., 30-m pixel size for the Landsat series). Our results demonstrate that traditional satellite-derived data products may not be sufficient to fully capture the fine-scale complexity in fire effects that are central to the ecological function of low,

moderate-, and mixed-severity fire (Furniss et al. 2020).

Post-fire mortality

The combination of fire, drought, and background mortality processes enhanced the importance of local stand structure as a mediator of mortality risk and provoked a strong spatial structure among medium- and large-diameter tree mortalities (Fig. 10). The post-disturbance mortality regime was not simply an extension of direct fire effects, nor was it a return to the pattern in pre-fire mortality (Figs. 3, 6). It was instead a novel regime that emerged from both additive and interactive effects of fire damage, drought, and background mortality agents. Second-order ecological interactions (e.g., bark beetles, mechanical failure, competition) were

important determinants of post-fire mortality (Table 1, Fig. 10), and the contagious nature of these mortality agents became evident at greater distances than pre-fire (Fig. 5). Local neighborhood structure assumed a central role in mediating overall mortality risk for all trees, and mortality risk of medium- and large-diameter trees became density-dependent (Figs. 7–9).

We speculate a few reasons for the amplified spatial structuring of post-fire mortality. First, contagious mortality processes may have been facilitated by the rapid pulse of fire-weakened trees, causing the pre-fire distribution of biotic mortality agents (bark beetles and pathogens) to become revealed. In other words, the fire may not have changed the spatial structure associated with these contagious agents, and it may have simply made their spatial structure more

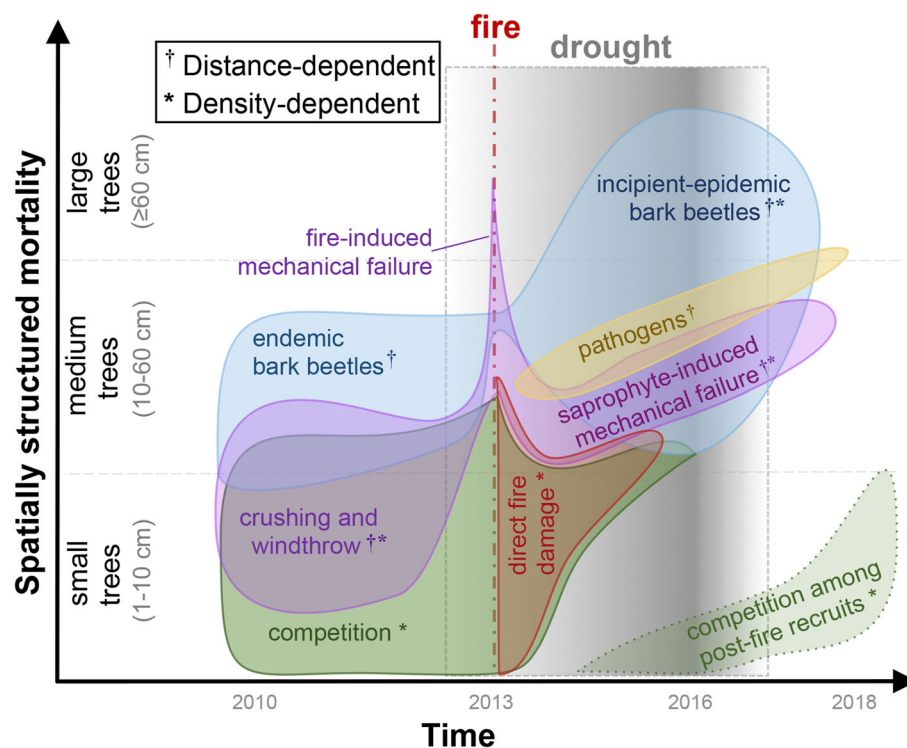


Fig. 10. Empirically informed conceptual model describing the development of spatially structured mortality processes before, during, and after compound disturbance (fire and drought). Polygons represent different mortality agents (colors match with Fig. 1). Position along the y-axis represents the tree diameters (cm DBH) for which each mortality process was spatially structured. The strength of each process (as detected in this study) is approximately related to polygon size. Superscripts indicate the form of spatial structuring (distance and/or density dependence) that was most evident for each process. Competition among post-fire recruitment was not analyzed in this study, but is shown in its hypothesized position.

evident. Alternatively, the post-fire proliferation of bark beetles and pathogens may have enhanced their ability to successfully attack most trees, enabling these mortality agents to kill trees that would have otherwise been resistant. This may have reduced the relative importance of individual tree characteristics (size, vigor, and defenses) and enhanced the importance of proximity to an infected host tree (i.e., distance dependence). In this case, the contagious nature of these mortality processes may have induced a pattern of aggregated mortality that would not have emerged in the absence of fire, even given enough time.

The elevated intensity of negative density dependence (Figs. 7–9) following fire may have also contributed to the increased scale of aggregation among contagious mortality agents. Despite the increased resource availability that would be expected due to direct fire mortality, surviving trees may not have been able to immediately utilize the newly available light, water, and soil resources. It can take years for trees to recover from direct fire damage (van Mantgem et al. 2011, Hood et al. 2018), and during this recuperative period, trees may have been particularly sensitive to density-dependent stress that could have increased susceptibility to drought, competition, and insect-related mortality (Kolb et al. 2007, Das et al. 2008, Yu et al. 2009, Anderegg et al. 2015, Clyatt et al. 2016, van Mantgem et al. 2016).

Fire also altered the diameter classes in which spatially structured mortality was most evident (Fig. 10). While pre- and direct fire mortality of small-diameter stems was aggregated, post-fire mortality of these trees became spatially random (Fig. 3). Conversely, the post-fire mortality regime induced a strong spatial structure among large-diameter mortalities that was not evident based on pre-fire or direct fire damage alone (Figs. 3, 6).

Distance-dependent post-fire mortality.—Bark beetles have long been a primary agent of large-diameter pine mortality in the Sierra Nevada (Das et al. 2016), and recent fire and drought events have stimulated a widespread increase in beetle-related mortality (van Mantgem et al. 2009, Stephenson et al. 2019). We observed an increase in both the rate and spatial scale of beetle-related mortality for medium- and large-

diameter *Abies* and *Pinus* post-fire (Table 1, Figs. 4, 5). The strong aggregation of large-diameter *Pinus* mortality (Fig. 5) is consistent with our expectations based on prior knowledge on beetle life history strategies and dispersal behavior (Furniss and Carolin 1977, Raffa et al. 2008), and this study offers a novel piece of quantitative evidence regarding the spatial extent of aggregation during a period of virulent beetle activity.

Beetle populations never reached epidemic levels at the YFDP, although they reached an intermediate point along the transition from endemic to epidemic beetle outbreaks known as the incipient-epidemic state. This is characterized by a transition of beetle host selection from weak trees to larger, vigorous, and more well-defended trees (Fig. 10; Safranyik and Carroll 2006, de la Mata et al. 2017, Stephenson et al. 2019), and it often spawns epidemic population levels that result in the decimation (>90% mortality) of the host species across broad landscapes (Safranyik and Carroll 2006, Raffa et al. 2008). Despite the increasing frequency of bark beetle epidemics in recent decades (Hicke et al. 2013), the factors governing the transition from endemic to epidemic population levels remain elusive, and beetle epidemics are notoriously difficult to predict (Peters et al. 2004, Raffa et al. 2008).

This study provides a relatively rare example (see Stephenson et al. 2019 for another) of a beetle outbreak that reached incipient-epidemic levels and then subsided back to endemic levels without first erupting into an epidemic. Total post-fire mortality of beetle-killed large-diameter *Pinus* was 36% (Table 1), but mortality returned to pre-fire rates as of 2019 (<1% per yr; data not shown). Two key factors likely contributed to the resistance of this forest to high-severity (>90% mortality) beetle outbreak: the high degree of structural and compositional heterogeneity due to centuries of low- to moderate-severity fire, and the wet winter of 2016–2017 that provided sudden relief from the extreme 2012–2015 drought (NOAA National Climate Data Center, <https://www.ncdc.noaa.gov>).

Despite the abundance of anecdotal knowledge that bark beetles attack and kill trees in clumps (Safranyik and Carroll 2006, Fettig et al. 2007, Graham et al. 2016, Fig. 1), few studies have explicitly quantified the fine-scale (<1 ha) spatial patterns associated with bark beetle

activity (due to both the contagious nature of beetle dispersal and density-dependent processes such as tree investment in defenses and beetle neighborhood selection). Most of the quantitative research regarding the spatial structure of bark beetle outbreaks has been conducted at intermediate to large spatial scales (1–10,000 ha, Fig. 1A; but see Bače et al. 2015 for a retrospective study at fine scales). We found that post-fire bark beetle mortality was aggregated at very fine scales (0–18 m) for large-diameter *Pinus*, and at slightly finer scales for medium-diameter *Abies* and *Pinus* (0–8 m and 0–12 m, respectively; Fig. 5). These different scales of aggregation may reflect differences in dispersal and aggregation strategy between the host-specific beetle species (primarily *Scolytus ventralis* LeConte for *Abies*; *Dendroctonus ponderosae* Hopkins and *Dendroctonus valens* LeConte for *Pinus*), as well as differences in the spatial pattern and neighborhood characteristics around medium- vs. large-diameter stems (Figs. 2, 3; see also Lutz et al. 2012).

Post-fire mechanical mortality of medium-diameter *Abies* (Fig. 5) was aggregated, a pattern that may have been driven by patches of windthrow in areas exposed to stronger winds (or less stable soil), as well as the crushing of small stems by individual large trees falling. There was a high rate of co-occurrence between saprophytic fungus and mechanical failure (56% of all *Abies* mechanical mortalities were mediated by wood decay in fire-killed portions of the stem), so the spatial pattern of mechanical mortality may have also been related to the distribution of saprophytic fungi (Fig. 10). These results are consistent with previous studies that have identified physical damage as an important mechanism of spatially non-random mortality in unburned, old-growth forests (Das et al. 2008, 2016, Larson and Franklin 2010), and it reveals mechanical mortality as a driver of spatially non-random mortality in post-fire forests as well.

In contrast to the spatial structure of pre-fire pathogen mortality, pathogen-related *Abies* mortality was slightly aggregated post-fire (Fig. 5). The elevated mortality rates post-fire (Table 1) may have facilitated the detection of non-random pathogen mortality that was present but undetectable pre-fire, or the fire may have weakened trees and facilitated pathogen-related mortality

among trees that would have tolerated pathogen infestation if the fire had not occurred.

Density-dependent post-fire mortality.—Fire increased the strength of density dependence, particularly for medium- and large-diameter conifers (Figs. 7–9, Table 2; Appendix S1: Table S4). As the post-fire mortality models controlled for CVS and DBH, this result does not simply reflect the first-order effects of forest structure on fire intensity (Fig. 2). Rather, delayed mortality was more likely mediated by density-dependent processes such as competition, drought stress, and susceptibility to biotic mortality agents (Fig. 10). While we cannot disentangle the relative influence of each mechanism, the frequency with which BA was the most important local neighborhood variable (Table 2) suggests that asymmetric competition from medium- and large-diameter trees was an important factor governing density-dependent mortality pressure post-fire (sensu Lutz et al. 2014, van Mantgem et al. 2018).

For *Abies*, the importance of non-species-specific neighborhood metrics (i.e., density and BA of all species combined, Table 1) suggests that density-dependent mortality pressure was conferred by intense competition from both conspecific and heterospecific neighbors. There was a strong positive relationship between large neighbors and mortality risk for *Abies* of all sizes (Fig. 7; Appendix S1: Table S4). Surprisingly, we also observed a negative relationship (i.e., positive density dependence–mortality risk decreases with increasing density) between density of surviving stems and mortality risk for medium-diameter *Abies* (Fig. 7). This positive density dependence may have emerged because survival of immediate fire effects was highest in mesic areas where fire intensity was lowest (Fig. 2), and these sites may have buffered the medium-diameter *Abies* from competition and drought stress post-fire.

For medium- and large-diameter *Pinus*, conversely, neighborhood composition was an important component of post-fire density dependence. The strongest predictor variable for these stems was a conspecific BA (Table 2; Appendix S1: Table S4), a result that reflects the importance of host-specific bark beetles as a primary determinant of post-fire mortality (though see Das et al. 2008 for a similar result from

unburned forests). Conspecific density may have elevated mortality risk by reducing trees' capacity to invest in resin defenses due to elevated competitive stress associated with strong intraspecific competition (Kolb et al. 1998, Hood and Sala 2015, de la Mata et al. 2017), and this may have increased susceptibility to bark beetles. Optimal host selection provides an additional explanation for this pattern of strong CNDD (i.e., mortality risk increases with more conspecifics): Beetle populations proliferated 2–3 yr post-fire (when drought intensity peaked), and this may have enabled beetles to selectively attack larger and more vigorous host trees (Fig. 10; Boone et al. 2011, Stephenson et al. 2019). As conspecific BA is tightly correlated with the abundance of large *Pinus*, neighborhoods with high conspecific BA would have been preferentially selected by dispersing beetles (Safranyik and Carroll 2006, Barbosa et al. 2009) and this would increase post-fire mortality risk. These results demonstrate that fire and drought may not only make the effects of local neighborhood on bark beetle risk more pronounced, they may reverse the directionality of density dependence and thus fundamentally alter the consequence of mortality on forest spatial pattern (Fig. 8).

Implications for fire mortality models

Existing fire mortality models (e.g., FOFEM) predict mortality with a high degree of accuracy (Woolley et al. 2012, Grayson et al. 2017, Hood and Lutes 2017), but performance is inconsistent for large-diameter trees (Hood et al. 2007, Kane et al. 2017a, Furniss et al. 2019). These models perform best when direct fire damage is the primary driver of mortality (i.e., trees with high percent crown scorch), but large-diameter trees are rarely killed by fire damage alone. Our findings concur with the widespread understanding that large-diameter trees are instead more susceptible to the physical and biotic mortality agents (i.e., drought and bark beetles) that mediate delayed mortality post-fire (Hood et al. 2018), but these background mortality processes are not represented by the independent variables (i.e., crown scorch and DBH) used in most post-fire mortality models (Woolley et al. 2012, Grayson et al. 2017, Hood and Lutes 2017). Spatially structured delayed mortality processes thus contribute to spatially autocorrelated error that manifests as

patches of over- or under-predicted mortality within a stand (Furniss et al. 2019). The relative infrequency of large-diameter trees (e.g., ~1% of individuals; Lutz et al. 2018) allows total model accuracy to remain high, despite systematic error that emerges when predictions are aggregated at the stand level (Furniss et al. 2019).

Both types of error may be reduced by incorporating stand structure variables into mortality models to capture the density-dependent processes that regulate delayed mortality (Figs. 7–9, Table 2; Appendix S1: Table S4). The inclusion of structural variables would particularly enhance the capacity of fire mortality models to predict post-fire spatial pattern: The resulting mortality predictions would not only reflect the variability in first-order fire intensity, they would also capture spatial heterogeneity in mortality risk due to forest composition, structure, and spatial pattern. This would also enhance the utility of mortality models for estimating the effects of fire on carbon stocks, as large-diameter trees contribute disproportionately to forest biomass (Lutz et al. 2018), and accurately modeling their demography will reduce the uncertainty associated with landscape-scale carbon estimates (Lutz et al. 2017b, Stenzel et al. 2019).

CONCLUSIONS

This study is the first quantitative comparison of fine-scale patterns associated with background mortality processes both before and after acute disturbance. Our analysis of pre-fire mortality was consistent with the existing paradigm that density-dependent mortality within late-successional forests is most prominent among the smallest trees, while mortality of larger and older trees is less density-dependent. This lack of strong negative density dependence among large trees, however, should not be conflated with spatially random mortality; contagious mortality processes may provoke distance-dependent mortality (Clyatt et al. 2016), and local neighborhood can still moderate mortality risk (Das et al. 2008). Additionally, disturbance provoked strong density dependence among large-diameter trees (Fig. 10), further contradicting the widespread expectation that large tree mortality in old-growth forests is spatially random (Franklin et al. 2002, Aakala et al. 2012, Lintz et al. 2016).

The mortality regime that emerged post-fire was distinct from either background mortality or direct fire effects (Fig. 10). Distance- and density-dependent background mortality processes interacted with fire damage to introduce heterogeneity at finer scales compared fire alone, providing a key insight regarding the formation of the complex, multi-scale spatial structure characteristic of frequent-fire forests (Hessburg et al. 1999, van Wagtendonk and Fites-Kaufman 2006). Although the post-fire mortality regime may have been brief relative to the life span of mature trees, the synergistic effects of fire, drought, and background mortality processes will have enduring effects on the spatial pattern of large-diameter trees, and thus the forest as a whole. These findings provide a more mechanistic understanding of temperate forest spatial pattern dynamics, and they contribute to theoretical models describing disturbances and the maintenance of ecological heterogeneity (Paine and Levin 1981, Larson and Churchill 2012). The foundational importance of fine-scale heterogeneity (Hessburg et al. 2015, Kelly and Brotons 2017) and the ecological significance of large-diameter trees (Larson et al. 2013, Lutz et al. 2018) render background mortality processes, and the post-disturbance mortality regime that they moderate, acutely consequential to the structure, function, and spatial pattern of forests.

ACKNOWLEDGMENTS

Funding was provided by the Joint Fire Science Program (award 16–1-04–02), the National Park Service (Awards P14AC00122 and P14AC00197), the Ecology Center at Utah State University, and the Utah Agricultural Extension Station at Utah State University which has designated this as journal paper number #9190. We thank Yosemite National Park for logistical assistance and the Yosemite Forest Dynamics Plot field crews, students, and volunteers (listed individually at <http://yfdp.org>) for their work. We particularly thank Mark Swanson for his persistent commitment to the YFDP, Sara Germain for her helpful comments throughout the study, Nate Stephenson for his support of our work in the YFDP and for sharing an early version of the pathology examination protocol with us, and two anonymous reviewers for their suggestions on a previous version of this manuscript. This work was performed under National Park Service research permits YOSE-2010-SCI-0003, YOSE-2011-SCI-0015,

YOSE-2012-SCI-0061, YOSE-2013-SCI-0012, YOSE-2014-SCI-0005, YOSE-2015-SCI-0014, YOSE-2016-SCI-0006, YOSE-2017-SCI-0009, and YOSE-2018-SCI-0006 for study YOSE-0051. The Yosemite Forest Dynamics Plot was made possible by a grant from Jennifer Walston Johnson to the Smithsonian ForestGEO.

LITERATURE CITED

- Aakala, T., S. Fraver, B. J. Palik, and A. W. D'Amato. 2012. Spatially random mortality in old-growth red pine forests of northern Minnesota. *Canadian Journal of Forest Research* 42:899–907.
- Adler, P. B., D. Smull, K. H. Beard, R. T. Choi, T. Furniss, A. Kulmatiski, J. M. Meiners, A. T. Tredennick, and K. E. Veblen. 2018. Competition and coexistence in plant communities: Intraspecific competition is stronger than interspecific competition. *Ecology Letters* 21:1319–1329.
- Allen, C. D. 2007. Interactions across spatial scales among forest dieback, fire, and erosion in northern New Mexico landscapes. *Ecosystems* 10:797–808.
- Allen, C. D., et al. 2010. A global overview of drought and heat-induced tree mortality reveals emerging climate change risks for forests. *Forest Ecology and Management* 259:660–684.
- Allen, C. D., D. D. Breshears, and N. G. McDowell. 2015. On underestimation of global vulnerability to tree mortality and forest die-off from hotter drought in the Anthropocene. *Ecosphere* 6:1–55.
- Allen, E. A., D. J. Morrison, and G. W. Wallis. 1996. Common tree diseases of British Columbia. Canadian Forest Service, Pacific Forestry Centre, Victoria, British Columbia, Canada.
- Allen, C. D., M. Savage, D. A. Falk, K. F. Suckling, T. W. Swetnam, T. Schulke, P. B. Stacey, P. Morgan, M. Hoffman, and J. T. Klingel. 2002. Ecological restoration of southwestern ponderosa pine ecosystems: a broad perspective. *Ecological Applications* 12:1418–1433.
- Anderegg, W. R. L., et al. 2015. Tree mortality from drought, insects, and their interactions in a changing climate. *New Phytologist* 208:674–683.
- Bačar, R., M. Svoboda, P. Janda, R. C. Morrissey, J. Wild, J. L. Clear, V. Čada, and D. C. Donato. 2015. Legacy of pre-disturbance spatial pattern determines early structural diversity following severe disturbance in montane spruce forests. *PLOS ONE* 10:e0139214.
- Baddeley, A. J., P. J. Diggle, A. Hardegen, T. Lawrence, R. K. Milne, and G. Nair. 2014. On tests of spatial pattern based on simulation envelopes. *Ecological Monographs* 84:477–489.
- Baddeley, A., E. Rubak, and R. Turner. 2015. Spatial point patterns: methodology and applications with R. Chapman and Hall/CRC Press, London, UK.

- Baguskas, S. A., S. H. Peterson, B. Bookhagen, and C. J. Still. 2014. Evaluating spatial patterns of drought-induced tree mortality in a coastal California pine forest. *Forest Ecology and Management* 315:43–53.
- Barbosa, P., J. Hines, I. Kaplan, H. Martinson, A. Szczepaniec, and Z. Szendrei. 2009. Associational resistance and associational susceptibility: having right or wrong neighbors. *Annual Review of Ecology, Evolution, and Systematics* 40:1–20.
- Barth, M. A. F., A. J. Larson, and J. A. Lutz. 2015. A forest reconstruction model to assess changes to Sierra Nevada mixed-conifer forest during the fire suppression era. *Forest Ecology and Management* 354:104–118.
- Beh, M. M., M. R. Metz, K. M. Frangioso, and D. M. Rizzo. 2012. The key host for an invasive forest pathogen also facilitates the pathogen's survival of wildfire in California forests. *New Phytologist* 196:1145–1154.
- Belmecheri, S., F. Babst, E. R. Wahl, D. W. Stahle, and V. Trouet. 2016. Multi-century evaluation of Sierra Nevada snowpack. *Nature Climate Change* 6:2–3.
- Belote, T. R., A. J. Larson, and M. S. Dietz. 2015. Tree survival scales to community-level effects following mixed-severity fire in a mixed-conifer forest. *Forest Ecology and Management* 353:221–231.
- Bentz, B. J., J. Régnière, C. J. Fettig, E. M. Hansen, J. L. Hayes, J. A. Hicke, R. G. Kelsey, J. F. Negrón, and S. J. Seybold. 2010. Climate change and bark beetles of the western United States and Canada: direct and indirect effects. *BioScience* 60:602–613.
- Berner, L. T., B. E. Law, A. J. H. Meddens, and J. A. Hicke. 2017. Tree mortality from fires, bark beetles, and timber harvest during a hot and dry decade in the western United States (2003–2012). *Environmental Research Letters* 12:065005.
- Biging, G. S., and M. Dobbertin. 1992. A comparison of distance-dependent competition measures for height and basal area growth of individual conifer trees. *Forest Science* 38:695–720.
- Birch, J. D., J. A. Lutz, E. H. Hogg, S. W. Simard, R. Pelletier, G. H. LaRoi, and J. Karst. 2019a. Decline of an ecotone forest: 50 years of demography in the southern boreal forest. *Ecosphere* 10:e02698.
- Birch, J. D., J. A. Lutz, S. W. Simard, R. Pelletier, G. H. LaRoi, and J. Karst. 2019b. Density-dependent processes fluctuate over 50 years in an ecotone forest. *Oecologia* 191:909–918.
- Blomdahl, E. M., C. A. Kolden, A. J. H. Meddens, and J. A. Lutz. 2019. The importance of small fire refugia in the central Sierra Nevada, California, USA. *Forest Ecology and Management* 432:1041–1052.
- Boone, C. K., B. H. Aukema, J. Bohlmann, A. L. Carroll, and K. F. Raffa. 2011. Efficacy of tree defense physiology varies with bark beetle population density: a basis for positive feedback in eruptive species. *Canadian Journal of Forest Research* 41:1174–1188.
- Bragg, D. C., M. G. Shelton, and B. Zeide. 2003. Impacts and management implications of ice storms on forests in the southern United States. *Forest Ecology and Management* 186:99–123.
- Breshears, D. D., et al. 2005. Regional vegetation die-off in response to global-change-type drought. *Proceedings of the National Academy of Sciences USA* 102:15144–15148.
- Burnham, K. P., and D. R. Anderson. 1998. Model selection and multimodel inference: a practical information-theoretic approach. Second edition. Springer, New York, New York, USA.
- Byer, S., and Y. Jin. 2017. Detecting drought-induced tree mortality in Sierra Nevada forests with time series of satellite data. *Remote Sensing* 9:929.
- Cansler, C. A., D. McKenzie, and C. B. Halpern. 2018. Fire enhances the complexity of forest structure in alpine treeline ecotones. *Ecosphere* 9:e02091.
- Cansler, C. A., M. E. Swanson, T. J. Furniss, A. J. Larson, and J. A. Lutz. 2019. Fuel dynamics after reintroduced fire in an old-growth Sierra Nevada mixed-conifer forest. *Fire Ecology* 15:16.
- Caprio, A. C., and T. W. Swetnam. 1995. Historic fire regimes along an elevational gradient on the west slope of the Sierra Nevada, California. Pages 173–179. Missoula, MT: General Technical Report Int. United States Department of Agriculture Forest Service.
- Churchill, D. J., A. J. Larson, M. C. Dahlgreen, J. F. Franklin, P. F. Hessburg, and J. A. Lutz. 2013. Restoring forest resilience: from reference spatial patterns to silvicultural prescriptions and monitoring. *Forest Ecology and Management* 291:442–457.
- Clark, D. B., and D. A. Clark. 1996. Abundance, growth and mortality of very large trees in neotropical lowland rain forest. *Forest Ecology and Management* 80:235–244.
- Clyatt, K. A., J. S. Crotteau, M. S. Schaedel, H. L. Wiggins, H. Kelley, D. J. Churchill, and A. J. Larson. 2016. Historical spatial patterns and contemporary tree mortality in dry mixed-conifer forests. *Forest Ecology and Management* 361:23–37.
- Comita, L. S., H. C. Muller-Landau, S. Aguilar, and S. P. Hubbell. 2010. Asymmetric density dependence shapes species abundances in a tropical tree community. *Science* 329:330–332.
- Connell, J. H. 1971. On the role of natural enemies in preventing competitive exclusion in some marine animals and in rain forest trees. Pages 298–312 in P. J. Den Boer and G. R. Gradwell, editors. *Dynamics of populations*. Centre for Agricultural Publishing

- and Documentation, Wageningen, The Netherlands.
- Das, A., J. Battles, N. L. Stephenson, and P. J. van Mantgem. 2011. The contribution of competition to tree mortality in old-growth coniferous forests. *Forest Ecology and Management* 261:1203–1213.
- Das, A., J. Battles, P. J. van Mantgem, and N. L. Stephenson. 2008. Spatial elements of mortality risk in old-growth forests. *Ecology* 89:1744–1756.
- Das, A. J., A. J. Larson, and J. A. Lutz. 2018. Individual species–area relationships in temperate coniferous forests. *Journal of Vegetation Science* 29:317–324.
- Das, A. J., N. L. Stephenson, and K. P. Davis. 2016. Why do trees die? Characterizing the drivers of background tree mortality. *Ecology* 97:2616–2627.
- Das, A. J., N. L. Stephenson, A. Flint, T. Das, and P. J. van Mantgem. 2013. Climatic correlates of tree mortality in water- and energy-limited forests. *PLOS ONE* 8:e69917.
- de la Mata, R., S. Hood, and A. Sala. 2017. Insect outbreak shifts the direction of selection from fast to slow growth rates in the long-lived conifer *Pinus ponderosa*. *Proceedings of the National Academy of Sciences USA* 114:7391–7396.
- Detto, M., M. D. Visser, S. J. Wright, and S. W. Pacala. 2019. Bias in the detection of negative density dependence in plant communities. *Ecology Letters* 22:1923–1939.
- Diggle, P. 1985. A kernel method for smoothing point process data. *Journal of the Royal Statistical Society. Series C (Applied Statistics)* 34:138–147.
- Dobbertin, M., A. Baltensweiler, and D. Rigling. 2001. Tree mortality in an unmanaged mountain pine (*Pinus mugo* var. *uncinata*) stand in the Swiss National Park impacted by root rot fungi. *Forest Ecology and Management* 145:79–89.
- Fensham, R. J., and J. E. Holman. 1999. Temporal and spatial patterns in drought-related tree dieback in Australian savanna. *Journal of Applied Ecology* 36:1035–1050.
- Fettig, C. J., K. D. Klepzig, R. F. Billings, A. S. Munson, T. E. Nebeker, J. F. Negrón, and J. T. Nowak. 2007. The effectiveness of vegetation management practices for prevention and control of bark beetle infestations in coniferous forests of the western and southern United States. *Forest Ecology and Management* 238:24–53.
- Franklin, J. F., et al. 2002. Disturbances and structural development of natural forest ecosystems with silvicultural implications, using Douglas-fir forests as an example. *Forest Ecology and Management* 155:399–423.
- Franklin, J. F., and K. N. Johnson. 2012. A restoration framework for federal forests in the Pacific Northwest. *Journal of Forestry* 110:429–439.
- Franklin, J. F., H. Shugart, and M. E. Harmon. 1987. Tree death as an ecological process. *BioScience* 37:550–556.
- Furniss, R. L., and V. M. Carolin. 1977. Western forest insects. U.S. Department of Agriculture, Forest Service, Washington, D.C., USA.
- Furniss, T. J., V. R. Kane, A. J. Larson, and J. A. Lutz. 2020. Detecting tree mortality with Landsat-derived spectral indices: improving ecological accuracy by examining uncertainty. *Remote Sensing of Environment* 237:111497. <https://doi.org/10.1016/j.rse.2019.111497>.
- Furniss, T. J., A. J. Larson, V. R. Kane, and J. A. Lutz. 2019. Multi-scale assessment of post-fire tree mortality models. *International Journal of Wildland Fire* 28:46–61. <https://doi.org/10.1071/WF18031>.
- Furniss, T. J., A. J. Larson, and J. A. Lutz. 2017. Reconciling niches and neutrality in a subalpine temperate forest. *Ecosphere* 8:e01847.
- Gendreau-Berthiaume, B., S. E. Macdonald, and J. J. Stadt. 2016. Extended density-dependent mortality in mature conifer forests: causes and implications for ecosystem management. *Ecological Applications* 26:1486–1502.
- Goheen, D. J., and E. M. Hansen. 1993. Effects of pathogens and bark beetles on forests. In T. D. Schowalter and G. M. Filip, editors. *Beetle-pathogen interactions in conifer forests*. Academic Press, London, UK.
- Goreaud, F., and R. Pélissier. 2003. Avoiding misinterpretation of biotic interactions with the intertype K12-function: population independence vs. random labelling hypotheses. *Journal of Vegetation Science* 14:681–692.
- Grabarnik, P., M. Myllymäki, and D. Stoyan. 2011. Correct testing of mark independence for marked point patterns. *Ecological Modelling* 222:3888–3894.
- Graham, R. T., L. A. Asherin, M. A. Battaglia, T. B. Jain, and S. A. Mata. 2016. Mountain pine beetles: a century of knowledge, control attempts, and impacts central to the Black Hills. General Technical Report RMRS-GTR-353. U.S. Department of Agriculture, Forest Service, Rocky Mountain Research Station, Fort Collins, Colorado, USA.
- Gray, L., and F. He. 2009. Spatial point-pattern analysis for detecting density-dependent competition in a boreal chronosequence of Alberta. *Forest Ecology and Management* 259:98–106.
- Grayson, L. M., R. A. Progar, and S. M. Hood. 2017. Predicting post-fire tree mortality for 14 conifers in the Pacific Northwest, USA: model evaluation, development, and thresholds. *Forest Ecology and Management* 399:213–226.
- Greenwood, D. L., and P. J. Weisberg. 2008. Density-dependent tree mortality in pinyon-juniper

- woodlands. *Forest Ecology and Management* 255:2129–2137.
- Grelen, H. E. 1983. May burning favors survival and early height growth of longleaf pine seedlings. *Southern Journal of Applied Forestry* 7:16–20.
- Guarín, A., and A. H. Taylor. 2005. Drought triggered tree mortality in mixed conifer forests in Yosemite National Park, California, USA. *Forest Ecology and Management* 218:229–244.
- Harris, L., and A. H. Taylor. 2015. Topography, fuels, and fire exclusion drive fire severity of the Rim fire in an old-growth mixed-conifer forest, Yosemite National Park, USA. *Ecosystems* 18:1192–1208.
- He, F., and R. P. Duncan. 2000. Density-dependent effects on tree survival in an old-growth Douglas-fir forest. *Journal of Ecology* 88:676–688.
- Hegyi, F. 1974. A simulation model for managing jack-pine stands. Pages 74–90 in J. Fries, editor. *Growth models for tree and stand simulation*. Royal College of Forestry, Stockholm, Sweden.
- Hermes, D. A., and W. J. Mattson. 1992. The dilemma of plants: to grow or defend. *Quarterly Review of Biology* 67:283–335.
- Hessburg, P. F., et al. 2015. Restoring fire-prone Inland Pacific landscapes: seven core principles. *Landscape Ecology* 30:1805–1835.
- Hessburg, P. F., J. K. Agee, and J. F. Franklin. 2005. Dry forests and wildland fires of the inland Northwest USA: contrasting the landscape ecology of the pre-settlement and modern eras. *Forest Ecology and Management* 211:117–139.
- Hessburg, P. F., B. G. Smith, and R. B. Salter. 1999. Detecting change in forest spatial patterns from reference conditions. *Ecological Applications* 9:1232–1252.
- Hicke, J. A., A. J. H. Meddens, C. D. Allen, and C. A. Kolden. 2013. Carbon stocks of trees killed by bark beetles and wildfire in the western United States. *Environmental Research Letters* 8:035032.
- Hiers, J. K., J. J. O'Brien, R. J. Mitchell, J. M. Grego, and E. L. Loudermilk. 2009. The wildland fuel cell concept: an approach to characterize fine-scale variation in fuels and fire in frequently burned longleaf pine forests. *International Journal of Wildland Fire* 18:315–325.
- Hille Ris Lambers, J., J. S. Clark, and B. Beckage. 2002. Density-dependent mortality and the latitudinal gradient in species diversity. *Nature* 417:732–735.
- Hood, S. M., S. Baker, and A. Sala. 2016. Fortifying the forest: Thinning and burning increase resistance to a bark beetle outbreak and promote forest resilience. *Ecological Applications* 26:1984–2000.
- Hood, S., and B. Bentz. 2007. Predicting postfire Douglas-fir beetle attacks and tree mortality in the northern Rocky Mountains. *Canadian Journal of Forest Research* 37:1058–1069.
- Hood, S. M., and D. Lutes. 2017. Predicting post-fire tree mortality for 12 Western US conifers using the First Order Fire Effects Model (FOFEM). *Fire Ecology* 13:66–84.
- Hood, S. M., C. W. McHugh, K. C. Ryan, E. Reinhardt, and S. L. Smith. 2007. Evaluation of a post-fire tree mortality model for western USA conifers. *International Journal of Wildland Fire* 16:679–689.
- Hood, S. M., and A. Sala. 2015. Ponderosa pine resin defenses and growth: metrics matter. *Tree Physiology* 35:1223–1235.
- Hood, S., A. Sala, E. K. Heyerdahl, and M. Boutin. 2015. Low-severity fire increases tree defense against bark beetle attacks. *Ecology* 96:1846–1855.
- Hood, S. M., J. M. Varner, P. van Mantgem, and C. A. Cansler. 2018. Fire and tree death: understanding and improving modeling of fire-induced tree mortality. *Environmental Research Letters* 13:113004.
- Hurst, J. M., G. H. Stewart, G. L. W. Perry, S. K. Wiser, and D. A. Norton. 2012. Determinants of tree mortality in mixed old-growth *Nothofagus* forest. *Forest Ecology and Management* 270:189–199.
- Janzen, D. H. 1970. Herbivores and the number of tree species in tropical forests. *American Naturalist* 104:501–528.
- Jeronimo, S. M. A., V. R. Kane, D. J. Churchill, J. A. Lutz, M. P. North, G. P. Asner, and J. F. Franklin. 2019. Forest structure and pattern vary by climate and landform across active-fire landscapes in the montane Sierra Nevada. *Forest Ecology & Management* 437:70–86.
- Jeronimo, S. M. A., J. A. Lutz, V. R. Kane, A. J. Larson, and J. F. Franklin. 2020. Burn weather and three-dimensional fuel structure determine post-fire tree mortality. *Landscape Ecology* 35:859–878.
- Johnson, D. J., N. A. Bourg, R. Howe, W. J. McShea, A. Wolf, and K. Clay. 2014. Conspecific negative density-dependent mortality and the structure of temperate forests. *Ecology* 95:2493–2503.
- Kane, J. M., P. J. van Mantgem, L. B. Lalemand, and M. Keifer. 2017a. Higher sensitivity and lower specificity in post-fire mortality model validation of 11 western US tree species. *International Journal of Wildland Fire* 26:444–454.
- Kane, J. M., J. M. Varner, M. R. Metz, and P. J. van Mantgem. 2017b. Characterizing interactions between fire and other disturbances and their impacts on tree mortality in western U.S. Forests. *Forest Ecology and Management* 405:188–199.
- Kane, V. R., C. A. Cansler, N. A. Povak, J. T. Kane, R. J. McGaughey, J. A. Lutz, D. J. Churchill, and M. P. North. 2015. Mixed severity fire effects within the Rim fire: relative importance of local climate, fire

- weather, topography, and forest structure. *Forest Ecology and Management* 358:62–79.
- Kane, V. R., J. A. Lutz, S. L. Roberts, D. F. Smith, R. J. McGaughey, N. A. Povak, and M. L. Brooks. 2013. Landscape-scale effects of fire severity on mixed-conifer and red fir forest structure in Yosemite National Park. *Forest Ecology and Management* 287:17–31.
- Kane, V. R., M. P. North, J. A. Lutz, D. J. Churchill, S. L. Roberts, D. F. Smith, R. J. McGaughey, J. T. Kane, and M. L. Brooks. 2014. Assessing fire effects on forest spatial structure using a fusion of Landsat and airborne LiDAR data in Yosemite National Park. *Remote Sensing of Environment* 151:89–101.
- Keeler-Wolf, T., P. Moore, E. Reyes, J. Menke, D. Johnson, and D. Karavidas. 2012. Yosemite National Park vegetation classification and mapping project report. Fort Collins, CO: Natural Resources Technical Report. National Park Service.
- Kelly, L. T., and L. Brotons. 2017. Using fire to promote biodiversity. *Science* 355:1264–1265.
- Kenkel, N. C. 1988. Pattern of self-thinning in Jack pine: testing the random mortality hypothesis. *Ecology* 69:1017–1024.
- King, D. A. 1986. Tree form, height growth, and susceptibility to wind damage in *Acer saccharum*. *Ecology* 67:980–990.
- Kolb, T. E., J. K. Agee, P. Z. Fulé, N. G. McDowell, K. Pearson, A. Sala, and R. H. Waring. 2007. Perpetuating old ponderosa pine. *Forest Ecology and Management* 249:141–157.
- Kolb, T. E., K. M. Holmberg, M. R. Wagner, and J. E. Stone. 1998. Regulation of ponderosa pine foliar physiology and insect resistance mechanisms by basal area treatments. *Tree Physiology* 18:375–381.
- Kolden, C. A., J. A. Lutz, C. H. Key, J. T. Kane, and J. W. van Wagten. 2012. Mapped versus actual burned area within wildfire perimeters: characterizing the unburned. *Forest Ecology and Management* 286:38–47.
- Kuuluvainen, T., and S. Rouvinen. 2000. Post-fire understorey regeneration in boreal *Pinus sylvestris* forest sites with different fire histories. *Journal of Vegetation Science* 11:801–812.
- LaManna, J. A., et al. 2017. Plant diversity increases with the strength of negative density dependence at the global scale. *Science* 356:1389–1392.
- Larson, A. J., R. T. Belote, C. A. Cansler, S. A. Parks, and M. S. Dietz. 2013. Latent resilience in ponderosa pine forest: effects of resumed frequent fire. *Ecological Applications* 23:1243–1249.
- Larson, A. J., C. A. Cansler, S. G. Cowdery, S. Hiebert, T. J. Furniss, M. E. Swanson, and J. A. Lutz. 2016. Post-fire morel (*Morchella*) mushroom abundance, spatial structure, and harvest sustainability. *Forest Ecology and Management* 377:16–25.
- Larson, A. J., and D. Churchill. 2012. Tree spatial patterns in fire-frequent forests of western North America, including mechanisms of pattern formation and implications for designing fuel reduction and restoration treatments. *Forest Ecology and Management* 267:74–92.
- Larson, A. J., and J. F. Franklin. 2010. The tree mortality regime in temperate old-growth coniferous forests: the role of physical damage. *Canadian Journal of Forest Research* 40:2091–2103.
- Larson, A. J., J. A. Lutz, D. C. Donato, J. A. Freund, M. E. Swanson, J. HilleRisLambers, D. G. Sprugel, and J. F. Franklin. 2015. Spatial aspects of tree mortality strongly differ between young and old-growth forests. *Ecology* 96:2855–2861.
- Linares, J. C., L. Taïqui, and J. J. Camarero. 2011. Increasing drought sensitivity and decline of Atlas cedar (*Cedrus atlantica*) in the Moroccan Middle Atlas forests. *Forests* 2:777–796.
- Lintz, H. E., A. N. Gray, A. Yost, R. Snieszko, C. Woodall, M. Reilly, K. Hutten, and M. Elliott. 2016. Quantifying density-independent mortality of temperate tree species. *Ecological Indicators* 66:1–9.
- Little, L. R. 2002. Investigating competitive interactions from spatial patterns of trees in multispecies boreal forests: the random mortality hypothesis revisited. *Canadian Journal of Botany* 80:93–100.
- Lorio, P. L. 1986. Growth-differentiation balance: a basis for understanding southern pine beetle-tree interactions. *Forest Ecology and Management* 14:259–273.
- Loudermilk, E. L., J. J. O'Brien, R. J. Mitchell, W. P. Cropper, J. K. Hiers, S. Grunwald, J. Grego, and J. C. Fernandez-Diaz. 2012. Linking complex forest fuel structure and fire behaviour at fine scales. *International Journal of Wildland Fire* 21:882–893.
- Lung-Escarmant, B., and D. Guyon. 2004. Temporal and spatial dynamics of primary and secondary infection by *Armillaria ostoyae* in a *Pinus pinaster* plantation. *Phytopathology* 94:125–131.
- Lutz, J. A. 2015. The evolution of long-term data for forestry: large temperate research plots in an era of global change. *Northwest Science* 89:255–269.
- Lutz, J. A., et al. 2018. Global importance of large-diameter trees. *Global Ecology and Biogeography* 27:849–864.
- Lutz, J. A., T. J. Furniss, S. J. Germain, K. M. L. Becker, E. M. Blomdahl, S. M. A. Jeronimo, C. A. Cansler, J. A. Freund, M. E. Swanson, and A. J. Larson. 2017a. Shrub communities, spatial patterns, and shrub-mediated tree mortality following reintroduced fire in Yosemite National Park, California, USA. *Fire Ecology* 13:104–126.

- Lutz, J. A., J. Matchett, L. Tarnay, D. Smith, K. M. L. Becker, T. J. Furniss, and M. Brooks. 2017b. Fire and the distribution and uncertainty of carbon sequestered as aboveground tree biomass in Yosemite and Sequoia & Kings Canyon National Parks. *Land* 6:10.
- Lutz, J. A., and C. B. Halpern. 2006. Tree mortality during early forest development: a long-term study of rates, causes, and consequences. *Ecological Monographs* 76:257–275.
- Lutz, J. A., A. J. Larson, T. J. Furniss, D. C. Donato, J. A. Freund, M. E. Swanson, K. J. Bible, J. Chen, and J. F. Franklin. 2014. Spatially nonrandom tree mortality and ingrowth maintain equilibrium pattern in an old-growth *Pseudotsuga-Tsuga* forest. *Ecology* 95:2047–2054.
- Lutz, J. A., A. J. Larson, M. E. Swanson, and J. A. Freund. 2012. Ecological importance of large-diameter trees in a temperate mixed-conifer forest. *PLOS ONE* 7:e36131.
- Lydersen, J. M., M. P. North, and B. M. Collins. 2014. Severity of an uncharacteristically large wildfire, the Rim Fire, in forests with relatively restored frequent fire regimes. *Forest Ecology and Management* 328:326–334.
- McCarley, T. R., C. A. Kolden, N. M. Vaillant, A. T. Hudak, A. M. S. Smith, and J. Kreidler. 2017. Landscape-scale quantification of fire-induced change in canopy cover following mountain pine beetle outbreak and timber harvest. *Forest Ecology and Management* 391:164–175.
- McDowell, N., et al. 2008. Mechanisms of plant survival and mortality during drought: Why do some plants survive while others succumb to drought? *New Phytologist* 178:719–739.
- McHUGH, C. W., and T. E. Kolb. 2003. Ponderosa pine mortality following fire in northern Arizona. *International Journal of Wildland Fire* 12:245.
- McMahon, S. M., G. Arellano, and S. J. Davies. 2019. The importance and challenges of detecting changes in forest mortality rates. *Ecosphere* 10: e02615.
- Meddens, A. J. H., J. A. Hicke, and C. A. Ferguson. 2012. Spatiotemporal patterns of observed bark beetle-caused tree mortality in British Columbia and the western United States. *Ecological Applications* 22:1876–1891.
- Meddens, A. J. H., C. A. Kolden, J. A. Lutz, J. T. Abatzoglou, and A. T. Hudak. 2018a. Spatiotemporal patterns of unburned areas within fire perimeters in the northwestern United States from 1984 to 2014. *Ecosphere* 9:e02029.
- Meddens, A. J. H., C. A. Kolden, J. A. Lutz, A. M. S. Smith, C. A. Cansler, J. T. Abatzoglou, G. W. Meigs, W. M. Downing, and M. A. Krawchuk. 2018b. Fire refugia: What are they, and why do they matter for global change? *BioScience* 68:944–954.
- Michaletz, S. T., and E. A. Johnson. 2006. A heat transfer model of crown scorch in forest fires. *Canadian Journal of Forest Research* 36:2839–2851.
- Michaletz, S. T., and E. A. Johnson. 2008. A biophysical process model of tree mortality in surface fires. *Canadian Journal of Forest Research* 38:2013–2029.
- Miller, C., and D. L. Urban. 1999a. A model of surface fire, climate and forest pattern in the Sierra Nevada, California. *Ecological Modelling* 114: 113–135.
- Miller, C., and D. L. Urban. 1999b. Interactions between forest heterogeneity and surface fire regimes in the southern Sierra Nevada. *Canadian Journal of Forest Research* 29:202–212.
- Miller, C., and D. L. Urban. 2000a. Modeling the effects of fire management alternatives on Sierra Nevada mixed-conifer forests. *Ecological Applications* 10:85–94.
- Miller, C., and D. L. Urban. 2000b. Connectivity of forest fuels and surface fire regimes. *Landscape Ecology* 15:145–154.
- Miller, J. D., C. N. Skinner, H. D. Safford, E. E. Knapp, and C. M. Ramirez. 2012. Trends and causes of severity, size, and number of fires in northwestern California, USA. *Ecological Applications* 22:184–203.
- North, M. P., et al. 2019. Tamm review: reforestation for resilience in dry western U.S. forests. *Forest Ecology and Management* 432:209–224.
- North, M., J. Innes, and H. Zald. 2007. Comparison of thinning and prescribed fire restoration treatments to Sierran mixed-conifer historic conditions. *Canadian Journal of Forest Research* 37:331–342.
- Packer, A., and K. Clay. 2000. Soil pathogens and spatial patterns of seedling mortality in a temperate tree. *Nature* 404:278–281.
- Paine, R. T., and S. A. Levin. 1981. Intertidal landscapes: disturbance and the dynamics of pattern. *Ecological Monographs* 51:145–178.
- Paine, T. D., K. F. Raffa, and T. C. Harrington. 1997. Interactions among Scolytid bark beetles, their associated fungi, and live host conifers. *Annual Review of Entomology* 42:179–206.
- Parker, T. J., K. M. Clancy, and R. L. Mathiasen. 2006. Interactions among fire, insects and pathogens in coniferous forests of the interior western United States and Canada. *Agricultural and Forest Entomology* 8:167–189.
- Pasher, J., and D. J. King. 2006. Landscape fragmentation and ice storm damage in Eastern Ontario forests. *Landscape Ecology* 21:477–483.
- Peet, R. K., and N. L. Christensen. 1987. Competition and tree death. *BioScience* 37:586–595.

- Perry, D., H. Margolis, C. Choquette, R. Molina, and J. Trappe. 1989. Ectomycorrhizal mediation of competition between coniferous tree species. *New Phytologist* 112:501–511.
- Peters, D. P. C., R. A. Pielke, B. T. Bestelmeyer, C. D. Allen, S. Munson-McGee, and K. M. Havstad. 2004. Cross-scale interactions, nonlinearities, and forecasting catastrophic events. *Proceedings of the National Academy of Sciences USA* 101:15130–15135.
- Punchi-Manage, R., T. Wiegand, K. Wiegand, S. Getzin, A. Huth, C. V. S. Gunatilleke, and I. A. U. N. Gunatilleke. 2015. Neighborhood diversity of large trees shows independent species patterns in a mixed dipterocarp forest in Sri Lanka. *Ecology* 96:1823–1834.
- R Core Team. 2018. R: a language and environment for statistical computing. R Foundation for Statistical Computing, Vienna, Austria.
- Raffa, K. F. 2014. Terpenes tell different tales at different scales: glimpses into the chemical ecology of conifer – bark beetle – microbial interactions. *Journal of Chemical Ecology* 40:1–20.
- Raffa, K. F., B. H. Aukema, B. J. Bentz, A. L. Carroll, J. A. Hicke, M. G. Turner, and W. H. Romme. 2008. Cross-scale drivers of natural disturbances prone to Anthropogenic amplification: the dynamics of bark beetle eruptions. *BioScience* 58:501–517.
- Raffa, K. F., and A. A. Berryman. 1983. The role of host plant resistance in the colonization behavior and ecology of bark beetles (Coleoptera: Scolytidae). *Ecological Monographs* 53:27–49.
- Rajala, T., S. C. Olhede, and D. J. Murrell. 2018. When do we have the power to detect biological interactions in spatial point patterns? *Journal of Ecology* 107:711–721.
- Rebertus, A. J., T. Kitzberger, T. T. Veblen, and L. M. Roovers. 1997. Blowdown history and landscape patterns in the Andes of Tierra del Fuego, Argentina. *Ecology* 78:678–692.
- Rothermel, R. C. 1972. A mathematical model for predicting fire spread in wildland fuels. Research Paper INT-115. USDA Forest Service, Intermountain Research Station, Ogden, Utah, USA.
- Ryan, K. C., and G. D. Amman. 1996. Bark beetle activity and delayed tree mortality in the Greater Yellowstone Area following the 1988 fires. Pages 151–158 in R. E. Keane, K. C. Ryan, and S. W. Running, editors. *Ecological Implications of Fire in Greater Yellowstone Proceedings*. International Association Wildland Fire, Fairland, Washington, USA.
- Safford, H. D., J. T. Stevens, K. Merriam, M. D. Meyer, and A. M. Latimer. 2012. Fuel treatment effectiveness in California yellow pine and mixed conifer forests. *Forest Ecology and Management* 274:17–28.
- Safranyik, L., and A. L. Carroll. 2006. The biology and epidemiology of the mountain pine beetle in lodgepole pine forests. Pages 3–66 in L. Safranyik and W. R. Wilson, editors. *The mountain pine beetle: a synthesis of biology, management, and impacts on lodgepole pine*. Natural Resources Canada, Canadian Forest Service, Pacific Forestry Centre, Victoria, British Columbia, Canada.
- Schaedel, M. S., A. J. Larson, D. L. R. Affleck, R. T. Belote, J. M. Goodburn, D. K. Wright, and E. K. Sutherland. 2017. Long-term precommercial thinning effects on *Larix occidentalis* (western larch) tree and stand characteristics. *Canadian Journal of Forest Research* 47:861–874.
- Schmitt, C. L., and M. L. Tatum. 2008. The Malheur National Forest location of the world's largest living organism [the humungous fungus]. USDA Forest Service, Pacific Northwest Region. http://www.fs.usda.gov/Internet/FSE_DOCUMENTS/fsbdev3_033146.pdf
- Scholl, A. E., and A. H. Taylor. 2010. Fire regimes, forest change, and self-organization in an old-growth mixed-conifer forest, Yosemite National Park, USA. *Ecological Applications* 20:362–380.
- Scott, D. W., C. L. Schmitt, and L. H. Spiegel. 2002. Factors affecting survival of fire injured trees: a rating system for determining relative probability of survival of conifers in the Blue and Wallowa Mountains. Report No. BMPMSC-03-01. USDA Forest Service, Blue Mountains Pest Management Service Center, La Grande, Oregon, USA.
- Sieg, C. H., J. D. McMillin, J. F. Fowler, K. K. Allen, J. F. Negron, L. L. Wadleigh, J. A. Anhold, and K. E. Gibson. 2006. Best predictors for postfire mortality of ponderosa pine trees in the Intermountain West. *Forest Science* 52:718–728.
- Silver, E. J., S. Fraver, A. W. D'Amato, T. Aakala, and B. J. Palik. 2013. Long-term mortality rates and spatial patterns in an old-growth *Pinus resinosa* forest. *Canadian Journal of Forest Research* 43:809–816.
- Smith, A. M. S., et al. 2016. Towards a new paradigm in fire severity research using dose–response experiments. *International Journal of Wildland Fire* 25:158–166.
- Smith, A. M. S., et al. 2017. Effects of fire radiative energy density dose on *Pinus contorta* and *Larix occidentalis* seedling physiology and mortality. *International Journal of Wildland Fire* 26:82–94.
- Sprugel, D. G. 1976. Dynamic structure of wave-regenerated *Abies balsamea* forests in the North-Eastern United States. *Journal of Ecology* 64:889–911.

- Sprugel, D. G., and F. H. Bormann. 1981. Natural disturbance and the steady state in high-altitude balsam fir forests. *Science* 211:390–393.
- Stenzel, J. E., et al. 2019. Fixing a snag in carbon emissions estimates from wildfires. *Global Change Biology* 25:3985–3994.
- Stephens, S. L., B. M. Collins, C. J. Fettig, M. A. Finney, C. M. Hoffman, E. E. Knapp, M. P. North, H. Safford, and R. B. Wayman. 2018. Drought, tree mortality, and wildfire in forests adapted to frequent fire. *BioScience* 68:77–88.
- Stephenson, N. L., A. J. Das, N. J. Ampersee, B. M. Bulaon, and J. L. Yee. 2019. Which trees die during drought? The key role of insect host-tree selection. *Journal of Ecology* 107:2383–2401.
- Stephenson, N. L., and P. J. van Mantgem. 2005. Forest turnover rates follow global and regional patterns of productivity. *Ecology Letters* 8:524–531.
- Taylor, A. H. 1990. Disturbance and persistence of Sitka spruce (*Picea sitchensis* (Bong) Carr.) in coastal forests of the Pacific Northwest, North America. *Journal of Biogeography* 17:47–58.
- Taylor, A. H., and C. N. Skinner. 2003. Spatial patterns and controls on historical fire regimes and forest structure in the Klamath Mountains. *Ecological Applications* 13:704–719.
- Thaxton, J. M., and W. J. Platt. 2006. Small-scale fuel variation alters fire intensity and shrub abundance in a pine savanna. *Ecology* 87:1331–1337.
- Turner, M. G., and W. H. Romme. 1994. Landscape dynamics in crown fire ecosystems. *Landscape Ecology* 9:59–77.
- Turner, M. G., W. H. Romme, R. H. Gardner, and W. W. Hargrove. 1997. Effects of fire size and pattern on early succession in Yellowstone National Park. *Ecological Monographs* 67:411–433.
- Ulanova, N. G. 2000. The effects of windthrow on forests at different spatial scales: a review. *Forest Ecology and Management* 135:155–167.
- van Mantgem, P. J., et al. 2009. Widespread increase of tree mortality rates in the western United States. *Science* 323:521–524.
- van Mantgem, P. J., A. C. Caprio, N. L. Stephenson, and A. J. Das. 2016. Does prescribed fire promote resistance to drought in low elevation forests of the Sierra Nevada, California, USA? *Fire Ecology* 12:13–25.
- van Mantgem, P. J., D. A. Falk, E. C. Williams, A. J. Das, and N. L. Stephenson. 2018. Pre-fire drought and competition mediate post-fire conifer mortality in western U.S. National Parks. *Ecological Applications* 28:1730–1739.
- van Mantgem, P. J., J. C. B. Nesmith, M. Keifer, E. E. Knapp, A. Flint, and L. Flint. 2013. Climatic stress increases forest fire severity across the western United States. *Ecology Letters* 16:1151–1156.
- van Mantgem, P. J., N. L. Stephenson, E. Knapp, J. Battles, and J. E. Keeley. 2011. Long-term effects of prescribed fire on mixed conifer forest structure in the Sierra Nevada, California. *Forest Ecology and Management* 261:989–994.
- van Wagtendonk, J. W., and J. Fites-Kaufman. 2006. Sierra Nevada Bioregion. Pages 264–294 in *Fire in California's ecosystems*. University of California Press, Berkeley, California, USA.
- Wang, X., L. S. Comita, Z. Hao, S. J. Davies, J. Ye, F. Lin, and Z. Yuan. 2012. Local-scale drivers of tree survival in a temperate forest. *PLOS ONE* 7: e29469.
- Waring, R. H., K. Cromack, P. A. Matson, R. D. Boone, and S. G. Stafford. 1987. Responses to pathogen-induced disturbance: decomposition, nutrient availability, and tree vigour. *Forestry* 60:219–227.
- Whitman, E., M.-A. Parisien, D. K. Thompson, R. J. Hall, R. S. Skakun, and M. D. Flannigan. 2018. Variability and drivers of burn severity in the northwestern Canadian boreal forest. *Ecosphere* 9: e02128.
- Wiegand, T., S. Gunatilleke, N. Gunatilleke, and T. Okuda. 2007. Analyzing the spatial structure of a Sri Lankan tree species with multiple scales of clustering. *Ecology* 88:3088–3102.
- Wiegand, T., and K. Moloney. 2004. Rings, circles, and null-models for point pattern analysis in ecology. *Oikos* 104:209–229.
- Wilson, M. F. J., B. O'Connell, C. Brown, J. C. Guinan, and A. J. Grehan. 2007. Multiscale terrain analysis of multibeam bathymetry data for habitat mapping on the Continental Slope. *Marine Geodesy* 30:3–35.
- Woolley, T., D. C. Shaw, L. M. Ganio, and S. Fitzgerald. 2012. A review of logistic regression models used to predict post-fire tree mortality of western North American conifers. *International Journal of Wildland Fire* 21:1–35.
- Yocom-Kent, L. L., P. Z. Fulé, W. A. Bunn, and E. G. Gdula. 2015. Historical high-severity fire patches in mixed-conifer forests. *Canadian Journal of Forest Research* 45:1587–1596.
- Yoda, K. 1963. Self-thinning in overcrowded pure stands under cultivated and natural conditions (Intraspecific competition among higher plants. XI). *Journal of the Institute of Polytechnics, Osaka City University Series D* 14:107–129.
- Young, D. J. N., J. T. Stevens, J. M. Earles, J. Moore, A. Ellis, A. L. Jirka, and A. M. Latimer. 2017. Long-term climate and competition explain forest mortality patterns under extreme drought. *Ecology Letters* 20:78–86.

- Youngblood, A., J. B. Grace, and J. D. McIver. 2009. Delayed conifer mortality after fuel reduction treatments: interactive effects of fuel, fire intensity, and bark beetles. *Ecological Applications* 19:321–337.
- Youngblood, A., T. Max, and K. Coe. 2004. Stand structure in eastside old-growth ponderosa pine forests of Oregon and northern California. *Forest Ecology and Management* 199:191–217.
- Yu, H., T. Wiegand, X. Yang, and L. Ci. 2009. The impact of fire and density-dependent mortality on the spatial patterns of a pine forest in the Hulun Buir sandland, Inner Mongolia, China. *Forest Ecology and Management* 257:2098–2107.
- Zhu, Y., J. A. Hogan, H. Cai, Y. Xun, F. Jiang, and G. Jin. 2017. Biotic and abiotic drivers of the tree growth and mortality trade-off in an old-growth temperate forest. *Forest Ecology and Management* 404:354–360.

DATA AVAILABILITY

The entire Yosemite Forest Dynamics Plot dataset is permanently archived and available through the Smithsonian ForestGEO Data Portal (<http://ctfs.si.edu/datarequest/>).

SUPPORTING INFORMATION

Additional Supporting Information may be found online at: <http://onlinelibrary.wiley.com/doi/10.1002/ecs2.3214/full>

SUPPORTING INFORMATION

Wildfire and drought moderate the spatial elements of tree mortality

Tucker J. Furniss^{1†}, Andrew J. Larson², Van R. Kane³, James A. Lutz¹

¹*Wildland Resources Department & Ecology Center, Utah State University, Logan, Utah*

²*Wilderness Institute & Department of Forest Management, University of Montana, Missoula, MT*

³*School of Environmental and Forest Sciences, University of Washington, Seattle, WA*

[†]Corresponding author email: tucker.furniss@usu.edu

Appendix S1 – Supplemental figures and tables and pathology exam data sheet

Supplemental figures

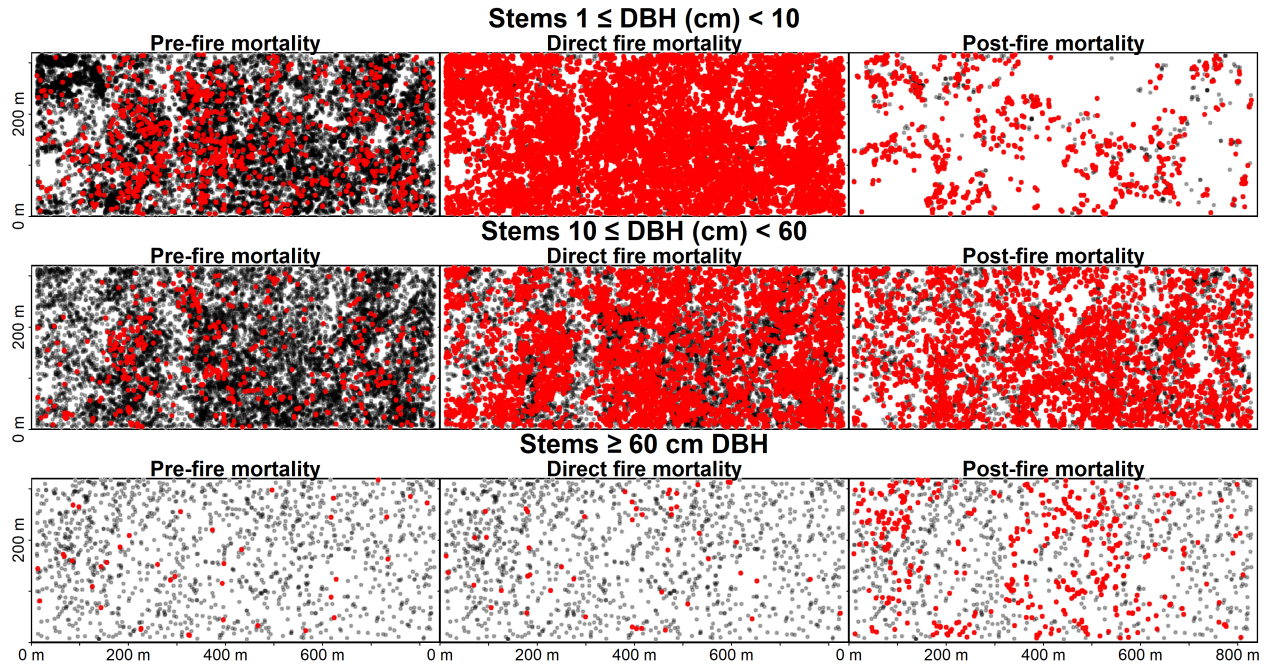


FIG S1. Stem maps of pre-fire, direct fire, and post-fire surviving stems (grey dots) and mortalities (red dots) within the Yosemite Forest Dynamics Plot. Maps correspond to the spatial pattern analysis presented in Fig. 6.

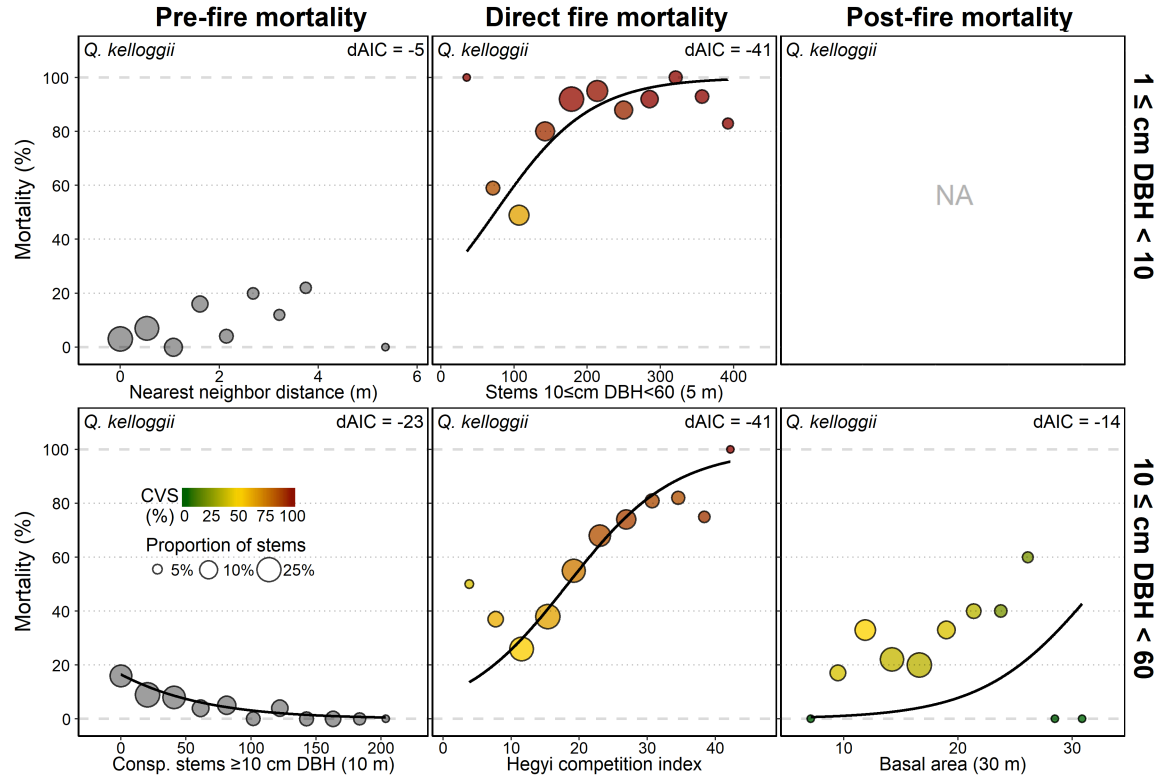


FIG. S2. Relationships between forest spatial structure and *Quercus kelloggii* mortality. Columns represent timing of mortality and rows represent tree diameter classes. Lines show the relationship between forest spatial structure and probability of mortality determined with generalized linear models. Points indicate observed proportion of mortality, and point size reflects relative number of stems in each group. The x-axis for each panel shows the single best structural variable for that mortality regime and size class; all variables may be found in Tables S2-S4. dAIC indicates the improvement in model accuracy compared to AIC of the non-spatial base model. Basal area (BA) is reported in $\text{m}^2 \text{ha}^{-1}$, stem categories are in stems ha^{-1} .

Supplemental tables

Table S1. Possible mechanisms of fire-related mortality. “Timing” indicates whether the mechanism of mortality is thought to be prevalent within 1 year of a fire (fire-related) or is a background mortality process that may be interact with fire to mediate post-fire mortality. “Susceptible stems” indicates the structural classes that are most susceptible to this form of mortality following low- to moderate-severity (i.e., non-crowning) fire; stems of other sizes may also be susceptible, just to a lesser degree. Relevant citations include studies that relate to each category of fire-related mortality; for a more extensive review of fire as a direct and indirect agent of tree mortality, see the recent review by Hood et al. (2018). Full citations are in Appendix C. For delayed mortality, we include relevant studies of tree mortality in the absence of fire as these ecological processes are also relevant in post-fire forests. The “Spatial metrics” columns represent the *categories* of local neighborhood variables which we hypothesize to be related to each mechanism of mortality, the *associated variables* that were calculated to reflect potential mortality mechanisms, and the *codes* representing each variable (codes relate to the results in Table S2). We calculated each structural variable for each tree within circular local neighborhoods with radii of 5, 10, 15, 20, and 30 m. In *codes*, “small” indicates stems 1 – 10 cm DBH, “med” indicates stems 10 – 60 cm DBH, “big” indicates stems ≥ 60 cm DBH, and “pole” indicates stems ≥ 10 cm DBH.

Timing	Mechanism of mortality	Susceptible stems	Relevant citations	Spatial metrics		
				Category	Associated variables	Codes
Fire-related	<i>Direct</i> ; fire damage	Small and medium stems	Ryan and Amman 1994, Sieg et al. 2006, Hood and Lutes 2017	Fuel loads, distribution, and fire-weather.	Density and basal area of local neighborhood. Nearest neighbor. Landscape position.	Den.small.neighbors; Den.med.neighbors; Den.big.neighbors; Den.neighbors;
	<i>Indirect</i> ; reduced resistance to fire damage	Small and medium stems	van Mantgem et al. 2013, Furniss et al. 2019	Competition. Drought.	Density and basal area of local neighborhood. Competition indices. Nearest neighbor. Landscape position.	BA; BA.conspecifics; Den.small.neighbors; Den.med.neighbors; Den.big.neighbors; Den.neighbors; HEGYI; INFLUENCE; Nearest.neighbor; LAND_POS;
	<i>Indirect</i> ; fire-related mechanical failure	Large stems (60+)	This study	Fire-scar (non-spatial)	Presence of fire scar (binary)	FIRE_SCAR;
Background mortality	<i>Bark-beetles</i>	Medium and large stems (i.e., “pole-sized”)	Ryan and Amman 1996, Hood and Bentz 2007, Hood et al. 2015, Kolb et al. 2007, Youngblood et al. 2009	Structure metrics for pole-sized conspecifics. Previous year beetle activity.	Density and basal area of surviving pole-sized and large conspecifics. Density of previous year beetle mortality	BA.surv.conspecifics; BA.surv.pole.con; BA.surv; Den.surv.conspecifics; Den.surv.pole.con; BA.prev.yr.beetle.mort; Den.prev.yr.beetle.mort;
	<i>Pathogens</i>	All	Parker et al. 2006, Das et al. 2016	Competition between surviving trees. Previous year pathogen activity.	Density and basal area of surviving trees. Competition indices for surviving trees. Density of previous year pathogen mortality	BA.surv; Den.surv.small.neighbors; Den.surv.med.neighbors; Den.surv.big.neighbors; Den.surv.neighbors; HEGYI.surv; Nearest.neighbor.surv; BA.prev.yr.fungal.mort; Den.prev.yr.fungal.mort;
	<i>Mechanical</i>	Medium and large stems	Das et al. 2016	Previous year pathogen activity. Fire-scar (non-spatial)	Density of previous year pathogen mortality. Presence of fire scar.	BA.prev.yr.fungal.mort; Den.prev.yr.fungal.mort; FIRE_SCAR;
	<i>Resource competition</i>	Small and medium stems	Das et al. 2008, Das et al. 2011, van Mantgem et al. 2018	Competition between surviving trees	Density and basal area of surviving trees. Competition indices for surviving trees. Nearest surviving neighbor.	BA.surv; Den.surv.small.neighbors; Den.surv.med.neighbors; Den.surv.big.neighbors; Den.surv.neighbors; HEGYI.surv; Nearest.neighbor.surv;
	<i>Drought</i>	All	van Mantgem and Stephenson 2007, van Mantgem et al. 2013, Furniss et al. 2019, van Mantgem et al. 2018, Stephens et al. 2018	Landscape position	Landscape position.	LAND_POS;

Table S2. Spatially-explicit forest structural attributes that were correlated with pre-fire mortality at $\alpha = 0.05$.

Significant correlations were identified by pairing each variable with a non-spatial, species-specific “base” model based on DBH. The following structural variables were significant at $\alpha = 0.05$ and improved AIC of the base model by >7 (delta AIC, “dAIC”, is reported for each structural variable). Grey text is used for the single best structural variable for mortality models that were not significantly enhanced by structural variables ($|dAIC| < 7$). Structural variables were summarized for each focal tree considering local neighborhood within 5, 10, 15, 20, and 30 m radii (all significant distances reported for each variable). Descriptions of the codes may be found in Table S1.

	Size	Pre-fire
<i>Abies concolor</i>	1-10	BA.30,20m;(-);dAIC=-53.4; BA.conspecifics.15,20,30,10,05m;(+)dAIC=-53.4; BA.pole.con.15,20,30,10,05m;(+)dAIC=-51.3; Den.big.neighbors.30,20,10,15,05m;(-);dAIC=-36.6; Den.med.neighbors.05,10,15,20,30m;(+)dAIC=-69.3; Den.neighbors.30,20,15m;(-);dAIC=-14.6; Den.pole.con.10,05,15,20,30m;(+)dAIC=-92.7; Den.small.neighbors.30,20,15,10,05m;(-);dAIC=-43.2
	10-60	BA.30,20,10,15m;(-);dAIC=-33; Den.big.neighbors.10,30m;(-);dAIC=-14.1; Den.neighbors.05,10m;(-);dAIC=-17.1; Den.small.neighbors.05,10,15m;(-);dAIC=-20; HEGYI (-);dAIC=-16; INFLUENCE (-);dAIC=-12.8; Nearest.neighbor (+);dAIC=-9.7
	≥ 60	Den.med.neighbors.10m;(-);dAIC=-5.4
<i>Calocedrus decurrens</i>	1-10	Den.neighbors.20m;(-);dAIC=-5.6
	10-60	Den.neighbors.30m;(-);dAIC=-3
	≥ 60	Den.med.neighbors.30m;(+)dAIC=-1.9
<i>Pinus lambertiana</i>	1-10	HEGYI (+);dAIC=-3.9
	10-60	Den.pole.con.20,15,30,10m;(-);dAIC=-9.8
	≥ 60	BA.pole.con.10m;(-);dAIC=-6.2
<i>Quercus kelloggii</i>	1-10	Nearest.neighbor (+);dAIC=-4.6
	≥ 10	BA.30m;(+)dAIC=-15.1; BA.conspecifics.05,10,15,20,30m;(-);dAIC=-15.1; BA.pole.con.05,10,15,20m;(-);dAIC=-12.1; Den.big.neighbors.30m;(+)dAIC=-8.3; Den.pole.con.10,20,15,05,30m;(-);dAIC=-22.9

Table S3. Spatially-explicit forest structural attributes that were correlated with direct and indirect immediate fire mortality at $\alpha = 0.05$. Significant correlations were identified by pairing each variable with non-spatial “base” models: “Direct fire” was based only on tree diameter (DBH), while “Indirect fire” was based on both DBH and crown volume scorched (CVS). The following structural variables were significant at $\alpha = 0.05$ and improved AIC of the base model by >7 (delta AIC, “dAIC”, is reported for each structural variable). Structural variables were summarized for each focal tree considering local neighborhood within 5, 10, 15, 20, and 30 m radii (all significant distances reported for each variable). Descriptions of the codes may be found in Table S1.

	Size	Direct fire		Indirect fire
<i>Abies concolor</i>	1-10	BA.05,10,15m;(+)dAIC=-125.4 BA.conspecifics.5,15,30,10,20m;(+)dAIC=-125.4 BA.pole.con.5,15,10,20,30m;(+)dAIC=-122.8 Den.big.neighbors.05,10m;(+)dAIC=-45.1 Den.big.neighbors.30,20m;(-)dAIC=-45.1 Den.med.neighbors.5,10,15,20,30m;(+)dAIC=-127.3 Den.neighbors.20m (+);dAIC=-14.4	Den.neighbors.30m (+);dAIC=-14.4 Den.pole.con.30,20,05,15,10m;(+)dAIC=-177.4 Den.small.neighbors.05,10m;(-);dAIC=-12.9 HEGYI (+);dAIC=-21.7 INFLUENCE (+);dAIC=-15.1 LAND_POS (+);dAIC=-72.3	Den.pole.con.05m;(+)dAIC=-4.4
	10-60	BA.20,15,30m;(-);dAIC=-99.6 BA.conspecifics.30,20,10,15,05m;(+)dAIC=-99.6 BA.pole.con.30,20,10,15,05m;(+)dAIC=-96.5 Den.big.neighbors.15,20,30,10m;(-);dAIC=-53.8 Den.med.neighbors.30,20,15m;(+)dAIC=-23.6 Den.neighbors.05m (-);dAIC=-7.8	Den.pole.con.30,20,15,10,05m;(+)dAIC=-31.5 Den.small.neighbors.05,10,15m;(-);dAIC=-16.8 HEGYI (+);dAIC=-36 INFLUENCE (+);dAIC=-27.1 LAND_POS (+);dAIC=-35.3 Nearest.neighbor (+);dAIC=-7.7	Den.small.neighbors.10m;(-);dAIC=-3.1
	≥60	Den.pole.con.30m;(+)dAIC=-6.3		—
<i>Calocedrus decurrens</i>	1-10	BA.conspecifics.30,20,15m;(-);dAIC=-23.4 BA.pole.con.30,20,15m;(-);dAIC=-24.7 Den.med.neighbors.20,15,30m;(+)dAIC=-10.9 INFLUENCE (+);dAIC=-9.4 LAND_POS (+);dAIC=-38.5		Den.small.neighbors.05m;(-);dAIC=-1.5
	10-60	BA.conspecifics.30,15,20m;(-);dAIC=-12.1 BA.pole.con.30,15,20m;(-);dAIC=-12.5		BA.05,15m;(+)dAIC=-70.1 BA.conspecifics.20m;(+)dAIC=-70.1 BA.pole.con.20m;(-);dAIC=-70.1 Den.med.neighbors.10m;(-);dAIC=-70.1 Den.small.neighbors.30m;(-);dAIC=-70.1 LAND_POS (-);dAIC=-70.1
	≥60	BA.30m;(-);dAIC=-5.8		
<i>Pinus lambertiana</i>	1-10	BA.05,10m;(+)dAIC=-22.1 BA.conspecifics.05,10,15m;(+)dAIC=-14.1 BA.pole.con.05,10,15m;(+)dAIC=-13.1 Den.big.neighbors.30m;(-);dAIC=-7.5	Den.med.neighbors.5,10,15,20,30m;(+)dAIC=-22.1 Den.pole.con.10,15,20,05m;(+)dAIC=-15 HEGYI (+);dAIC=-8.5 INFLUENCE (+);dAIC=-7.7	Den.big.neighbors.30m;(-);dAIC=-8.4 Den.med.neighbors.20,15,30,10m;(+)dAIC=-11.6
	10-60	Den.neighbors.05m (-);dAIC=-9.8 Den.small.neighbors.05,15,10m;(-);dAIC=-9.1		FIRE_SCAR (+);dAIC=-65.1
	≥60	BA.conspecifics.05m;(+)dAIC=-8.6 BA.pole.con.05m;(+)dAIC=-8.6 FIRE_SCAR (+);dAIC=-24		FIRE_SCAR (+);dAIC=-6.7
<i>Quercus kelloggii</i>	1-10	BA.20,15,30,10m;(+)dAIC=-27.1; BA.conspecifics.05,10,30m;(-);dAIC=-14.3; BA.pole.con.05,10,30m;(-);dAIC=-14.6; Den.big.neighbors.20,30m;(+)dAIC=-11.2;	Den.med.neighbors.15,20,10m;(+)dAIC=-41.4; Den.neighbors.10,15,20m (+);dAIC=-35.3; Den.pole.con.30m;(-);dAIC=-10.2; Den.small.neighbors.15,20m;(+)dAIC=-18	Den.neighbors.15m (+);dAIC=-8.5 Den.neighbors.20m (+);dAIC=-8.5 Den.small.neighbors.15,20,10m;(+)dAIC=-10.6
	≥10	BA.30,20m;(+)dAIC=-28.9 BA.conspecifics.10,15,30,05,20m;(-);dAIC=-26.6 BA.pole.con.10,15,30,20,05m;(-);dAIC=-28.9 Den.med.neighbors.20,15,30m;(+)dAIC=-22 Den.neighbors.15-30m (+);dAIC=-19.4 Den.pole.con.10,05,15,30,20m;(-);dAIC=-30.2	Den.small.neighbors.20m;(+)dAIC=-8.6 HEGYI (+);dAIC=-41.6 INFLUENCE (+);dAIC=-8.3	Den.neighbors.5,10,15,20,30m (+);dAIC=-17.8 Den.pole.con.05m;(-);dAIC=-7.5 Den.small.neighbors.5,10,15,20,30m;(+)dAIC=-19.6 HEGYI (+);dAIC=-17 LAND_POS (+);dAIC=-8.7

Table S4. Spatially-explicit forest structural attributes that were correlated with post-fire mortality at $\alpha = 0.05$.

Significant correlations were identified by pairing each variable with a non-spatial “base” model based on both DBH and crown volume scorched (CVS). The following structural variables were significant at $\alpha = 0.05$ and improved AIC of the base model by >7 (delta AIC, “dAIC”, is reported for each structural variable). Structural variables were summarized for each focal tree considering local neighborhood within 5, 10, 15, 20, and 30 m radii (all significant distances reported for each variable). Descriptions of the codes may be found in Table S1.

	Size	Post-fire		
<i>Abies concolor</i>	1-10	BA.05,10m;(+)dAIC=-48.9 BA.conspec.05m;(+)dAIC=-19 BA.mort.pole.con.05m;(+)dAIC=-7.2 BA.pole.con.05m;(+)dAIC=-17.7 BA.surv.05,10m;(+)dAIC=-45.8	BA.surv.conspec.05m;(+)dAIC=-16.8 BA.surv.pole.con.05m;(+)dAIC=-15.7 Den.big.neighbors.05m;(+)dAIC=-16.9 Den.med.neighbors.05,10m;(+)dAIC=-22.8 Den.pole.con.05,10m;(+)dAIC=-29	Den.surv.big.neighbors.5m;(+)dAIC=-16 Den.surv.med.neighbors.5,10,30m;(+)dAIC=-23.7 Den.surv.pole.con.05,10m;(+)dAIC=-26.4 Den.surv.small.neighbors.15,20,10m;(-)dAIC=-17.3
	10-60	BA.conspec.5-30m;(+)dAIC=-117.1 BA.05,10,15,30,20m;(+)dAIC=-117.1 BA.pole.con.5-30m ;(+)dAIC=-115.4 BA.surv.pole.con.5-30m ;(+)dAIC=-82.1 BA.surv.05,10,15,30,20m;(+)dAIC=-82.1	Den.big.neighbors.05,10m;(+)dAIC=-26.5 Den.mort.pole.con.5,10,15m (+)dAIC=-63.2 Den.mort.pole.con.20,30m (+)dAIC=-63.2 Den.pole.con.5,15,10,20,30m;(+)dAIC=-62.4 Den.surv.big.neighbors.05,10m;(+)dAIC=-27	Den.surv.small.neighbors.5-30m;(-)dAIC=-125.9; BA.mort.pole.con.5-30m ;(+)dAIC=-54.4 BA.surv.conspec.5-30m ;(+)dAIC=-80.3 Den.med.neighbors.5-30m ;(+)dAIC=-30.4 Den.small.neighbors.5-30m ;(-)dAIC=-23.7
	≥ 60	BA.30,20m;(+)dAIC=-12.4 BA.conspec.15,10,30m;(+)dAIC=-9.2 BA.pole.con.15,10m;(+)dAIC=-9.5 BA.surv.20,30m;(+)dAIC=-8.8	BA.surv.conspec.15m;(+)dAIC=-8.8 BA.surv.pole.con.15m;(+)dAIC=-8.8 HEGYI.surv (+)dAIC=-8.9	Den.big.neighbors.20,30,15,10m;(+)dAIC=-15.2 Den.surv.big.neighbors.20,30,15,10m;(+)dAIC=-12.9
<i>Calocedrus decurrens</i>	1-10	BA.20m;(+)dAIC=-13.9 BA.conspec.20,15m;(+)dAIC=-13.9 BA.pole.con.20,15m;(+)dAIC=-13.8	BA.surv.20,15m;(+)dAIC=-13.6 BA.surv.conspec.15,20m;(+)dAIC=-13.6 BA.surv.pole.con.15,20m;(+)dAIC=-13.4	Den.big.neighbors.20,15m;(+)dAIC=-7.4 Den.pole.con.20,15m;(+)dAIC=-9.9 Den.surv.big.neighbors.15,20m;(+)dAIC=-7.2 Den.surv.pole.con.20,15,10m;(+)dAIC=-13.1
	10-60	BA.conspec.05m;(+)dAIC=-6.7 BA.pole.con.05m;(+)dAIC=-7	BA.surv.conspec.05m;(+)dAIC=-7.7 BA.surv.pole.con.05m;(+)dAIC=-7.8	
	≥ 60	BA.30m;(+)dAIC=-2.8		
<i>Pinus lambertiana</i>	1-10	BA.surv.conspec.30m;(+)dAIC=-4.8		
	10-60	BA.05,10,30,20m;(+)dAIC=-37.2 BA.conspec.5-30m ;(+)dAIC=-37.1 BA.pole.con.5-30m ;(+)dAIC=-37.2 BA.surv.05,10,20m;(+)dAIC=-34.5	Den.surv.big.neighbors.05m;(+)dAIC=-21.5 Den.neighbors.20,30m;(+)dAIC=-10.3 Den.big.neighbors.5m;(+)dAIC=-20.4	BA.surv.conspec.5,10,15,20,30m;(+)dAIC=-34.3 BA.surv.pole.con.5,10,15,20,30m;(+)dAIC=-34.5 Den.med.neighbors.30,20,15m;(+)dAIC=-17.3 Den.pole.con.30,20,10,05,15m;(+)dAIC=-19.4
	≥ 60	Hegyi;(+)dAIC=-76.8 BA.5-30m;(+)dAIC=-64.2 BA.conspec.5-30m ;(+)dAIC=-63.1 BA.pole.con.5-30m ;(+)dAIC=-63.3 BA.surv.5-30m ;(+)dAIC=-64.2 BA.surv.conspec.5-30m;(+)dAIC=-64.2	BA.surv.pole.con.5-30m;(+)dAIC=-64.2 Den.big.neighbors.5-20m;(+)dAIC=-26.6 Den.med.neighbors.10-30m;(+)dAIC=-16.7 Den.neighbors.5-30m (+)dAIC=-65.4 Den.pole.con.5-30m (+)dAIC=-44.6	Den.surv.neighbors.5-30m;(+)dAIC=-58.3 Den.surv.pole.con.5-30m;(+)dAIC=-58.3 Den.small.neighbors.5,15,10,20,30m;(+)dAIC=-64.1 Den.surv.big.neighbors.5,15,10,20m;(+)dAIC=-28.5 Den.surv.med.neighbors.5-30m (+)dAIC=-39.8 BA.prev.yr.beetle.mort.5-30m (+)dAIC=-64.2
<i>Quercus kelloggii</i>	1-10	—	—	—
	≥ 10	BA.30,20m;(+)dAIC=-13.7 BA.surv.30m;(+)dAIC=-12	Den.med.neighbors.10-20m;(+)dAIC=-10.3 Den.surv.small.neighbors.20m;(-)dAIC=-8.9 HEGYI (+)dAIC=-12.6 HEGYI.surv (+)dAIC=-12.6	

Pathology exam data sheet

Western Forest Initiative Tree Pathology Exam Codes

Mortality Data

DBH: diameter at breast height (1.37 m); perpendicular to bole. Measure in cm to nearest mm.

Root condition

- 1 = Root-soil interface intact
- 2 = Root-soil interface damaged but stem still freestanding
- 3 = uprooted, stem no longer free standing.

Stem condition

- 1 = Main stem intact
- 2 = Main stem pinned or ruptured (e.g., crushed)
- 3 = Main stem snapped (no longer connected)

Snag height (m): Measure with laser to top of standing portion of the bole.

Snag top diameter (cm). If main stem is fully intact, record 0 cm. Otherwise, estimate to nearest 10 cm.

% Crown: Estimate percent of crown still intact. Do not enter values <100% for sparse crowns or gradual dieback.

% Tree: Estimate percent of the entire main stem length that is standing unbroken.

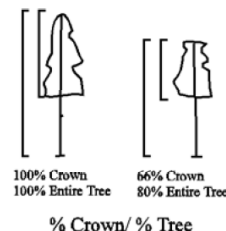
Leaner Angle: If tree is still rooted and is leaning, estimate the angle of lean in degrees from vertical (see diagram). Use this category for trees that are standing with crown and for trees that are crushed but still rooted.

% Ground: Estimate the percent of the down stem portion that is in direct contact with the ground.

% Supported: Estimate the percent of the down stem portion that is supported above ground. Use %Ground and %Supported only if %Crown and %Tree is less than 100% (and stem condition is 2 or 3). A tree that is crushed but still self-supported is not considered to be down. Only consider the down portion of the tree when estimating percent; %Ground and %Supported should add to 100%.

Special cases: If data can't be recorded, leave cell blank and note reason in comments. For example, if the top portion of the tree is broken off and can't be found, record data about the standing portion of the tree under STANDING and leave both columns of DOWN blank. Broken tops hung up in the canopy are considered down but supported. If tree cannot be found, look again (!); if all else fails comment "Tree not found" and list CC=38.

Comments: Record details regarding the condition codes and FADs



Tree Condition Codes

Crown

- 01 Dead needles or leaves present
- 02 Earlier loss of crown portion
- 03 Foliage Damage
- 04 Spike top/ top dieback
- 05 Crown flat topped
- 06 Mistletoe plants observed (use binoculars)
- 07 Witches brooms

Bole/Branches/Roots

- 13 Rotten wood
- 14 Mycelia/ rhizomorphs/ fungal fruiting body (non-conk)
- 15 Rot at break
- 16 Pitch tube on bole
- 17 Beetle galleries
- 18 Exit/entrance holes
- 19 Conks (indicate type and position)
- 20 Swelling
- 21 Canker
- 22 Evidence of scale (black bark)
- 23 Tree is hollow
- 24 Pitching
- 25 Pitch sheets
- 26 Oozing wounds
- 27 Bark sloughing
- 28 Scar on bole (note cause, location, extent)
- 29 Girdling (note cause)
- 30 Woodpecker/ Sapsucker activity (note extent)
- 31 Snow/ ice damage

Other

- 32 Uprooted or partially ruptured but foliage is still live.
- 35 Sprouting at base (if sprout is from same stem, use 37)
- 36 Tree dead several years (note reasoning, estimate years)
- 37 Tree dead above breast height, live below (if sprouting at base, use 35)
- 38 Tree not found

Factors Associated with Death (order by importance)

- 40 Unknown
- 68 Tree not found for ≥2 years in a row

Biotic

- 50 Suppression
- 51 Animal damage (specify animal if possible)
- 52 Mistletoe

Disease

- 61 White pine blister rust
- 62 Rot – specify in comments if possible
- 63 Canker
- 64 Other (specify)
- 65 Unknown

Insect

- 71 Bark (specify if possible)
- 72 Defoliating (specify if possible)
- 73 Other (specify)

Physical

- 80 Uprooted by falling tree or tree parts (note originating tree)
- 81 Uprooted (note cause)
- 82 Broken stem by falling tree or tree parts (partial or full crown loss)
- 83 Broken stem (entire or partial crown loss) (note cause)
- 84 Crown damage (stripped, broken branches, etc.)
- 85 Crushed by falling tree or tree parts (note originating tree)
- 86 Crushed (note cause)
- 87 Lightning
- 88 Other (note cause)
- 89 Tree located, physically removed from plot (e.g., landslide)

Fire

- 91 Crown scorch (killed by fire scorch, not consumption)
- 92 Crown combustion (note extent of consumption)
- 93 Bole/stem scorch (bark intact)
- 94 Bole/stem combustion (bark partially or entirely consumed)
- 95 Cambial heating (not scorched but heated to over 60°C)
- 96 Burned through at base (for small trees, due to litter & duff consumption around base)
- 97 Other (describe)
- 98 Fire, mechanical (fire burned base, but tree died because of structural failure. Tree would have survived if stem didn't break)
- 99 Complete consumption (<25% of stem remaining)

* Adapted from the tree pathology protocol developed by the USGS, Biological Resources Division, Sequoia & Kings Canyon and Yosemite National Parks